Magmatic silicate melts: Relations between bulk composition, structure and properties

BJORN O. MYSEN

Geophysical Laboratory, Carnegie Institution of Washington, Washington, D.C. 20008, U.S.A.

Abstract—Experimental data for silicate melt structure in iron-, phosphorous- and titanium-bearing binary metal oxide-silica and ternary metal oxide-alumina-silica systems have been employed to develop equations that describe the abundance of structural units as a function of bulk composition. These equations are used to describe the structures of natural magmatic liquids.

The structure of liquids for a collection of bulk chemical analyses of up to 2609 samples of Cenozoic volcanic rocks from rockfile RKNFSYS have been calculated. The degree of polymerization (nonbridging oxygens per tetrahedrally-coordinated cations, NBO/T) of natural magma is greater the more felsic the liquid with the NBO/T of rhyolite (from 367 analyses) = 0.031 ± 0.052, dacite (338 analyses) = 0.113 ± 0.040, andesite (2068 analyses) = 0.252 ± 0.123, tholeiite (1010 analyses) = 0.707 ± 0.250, alkali basalt (279 analyses) = 0.681 ± 0.264, basanite (206 analyses) = 0.808 ± 0.267 and nephelinite (116 analyses) = 0.909 ± 0.334. The principal structural unit in these liquids is that of a three-dimensional network (TO_2). Its abundance is positively correlated with decreasing NBO/T of the magma and ranges from an average near 50% for basaltic liquids to more than 95% for rhyolite. In all but rhyolitic and dacitic melts, the nonbridging oxygens are found predominantly in units with an average NBO/T = 2 (TO_3 units). In rhyolite and dacite, nonbridging oxygens occur mainly in structural units with NBO/T = 1 (T_2O_5 units). Units with NBO/T = 4 (TO_4 units) generally are present in all magmatic liquids and constitute between 10 and 20% of the structure in basaltic liquids.

Molar volume of natural magmatic liquids can be calculated from available experimental data. Molar volume of natural magmatic liquids is positively correlated with decreasing NBO/T and linearly correlated with the abundance of TO_2 units in the melts. Similar relationships exist for viscous properties. Both viscosity and activation energy of viscous flow, calculated with a selection of 2609 bulk chemical analyses, decrease with increasing NBO/T of the melt. As for molar volumes, the abundance of TO_2 units governs both the values of viscosity and activation energies of viscous flow. The values of these proportions appear insensitive to the mol fractions of TO_4 and T_2O_5 units in the magmatic liquids.

INTRODUCTION

THE STRUCTURE of magmatic liquids as a function of pressure, temperature and bulk composition provides a basis for characterization and prediction of the physical and chemical properties needed to describe magmatic processes. Largely as a result of extensive spectroscopic (Raman, infrared, Mossbauer, XRDF, EXAFS and XANES and NMR) studies of melt structure in binary, ternary and quarternary systems, the principal structural features likely to be encountered in the bulk compositional range of natural igneous rocks have been established. Direct determination of the structure of melts of natural igneous rock compositions generally has not been attempted (note, however, exceptions by SCARFE, 1977; HOCHELLA and BROWN, 1985). This lack of data results from limitations in resolution of spectra from melts and glasses of complex chemical systems such as natural rock compositions. This conclusion differs from that for simple binary metal oxide-silica systems where it is possible to establish the relative stability and abundance of specific structural units as a function of the type and concentration of network-modifying cations (*e.g.,* BRAWER and WHITE, 1975, 1977; VERWEIJ, 1979a,b; FURUKAWA *et al.,* 1981; MYSEN *et al.,* 1982). With more than one kind of network-modifying cations in a melt, such determinations are not possible because the structural tools are not sensitive to distinction between nonbridging oxygen bonded to specific network-modifying cations.

By addition of alumina to binary metal oxide systems, Al^{3+} generally occurs in tetrahedral coordination. In aluminosilicate melts with nonbridging oxygen Al^{3+} is distributed between the coexisting structural units (MYSEN *et al.,* 1985a; DOMINE and PIRIOU, 1986). In ternary metal oxide-alumina-silica systems, distribution coefficients for Al^{3+} between structural units may be estimated by monitoring frequency shifts of Raman bands resulting from Al^{3+} substitution for Si^{4+} (SEIFERT *et al.,* 1982; MCMILLAN *et al.,* 1982; MYSEN *et al.,* 1981a, 1985a) (Figure 1). The aluminum distribution between the structural units is, however, a function of the type of metal cation (MYSEN *et al.,* 1981a),
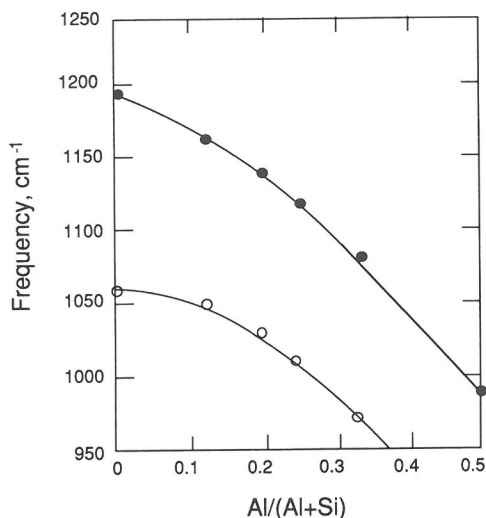
FIG. 1. Frequency shifts of (Si,Al)-O^0 stretch bands as a function of bulk melt Al/(Al + Si) for compositions on the join SiO_2-$NaAlO_2$ (data from SEIFERT et al., 1982).

but the structural tools are insufficiently sensitive to distinguish between Al^{3+} distribution governed by, for example, sodium and calcium if these two cations occur together in a melt. Both of these components play a major role in natural magmatic liquids.

Another important variable in igneous rocks is $Fe^{3+}/\Sigma Fe$, which from simple-system calibration is positively correlated with increasing oxygen fugacity, increasing total iron content, increasing Al/(Al + Si) and decreasing degree of polymerization. These relationships have been determined quantitatively in simple system melts by studying each effect separately (e.g., LAUER, 1977; DICKENSON and HESS, 1981, 1986; MYSEN et al., 1980a, 1984, 1985b; see also Figure 2). In natural magmatic systems, these individual effects are less clear (e.g., THORNBER et al., 1980; SACK et al., 1980; KILINC et al., 1983) because bulk compositional effects cannot be separated and experimentally observed variations in $Fe^{3+}/\Sigma Fe$ cannot be uniquely ascribed to a particular change in intensive or extensive variables.

Despite the complications summarized above, one of the goals in studying the structure of silicate melts in compositionally simple systems is to apply these results quantitatively to natural magmatic liquids. In the present report, available data that quantitatively relate bulk composition, temperature and oxygen fugacity to structure and properties of silicate melts in binary, ternary and quarternary systems will be described with the aid of equations

derived from the simple system structure data. These equations will then be used to calculate the structure of magmatic liquids from published major element compositions.

DATA BASE

Bulk chemical analyses

This report serves two purposes. First, a numerical description of the structural data base will be developed. Second, this data base will be used to describe the structure of natural magmatic liquid. This model will then be applied to a selection of rock analyses from a file of 16129 bulk chemical analyses of cenozoic extrusive rocks (RKNFSYS) compiled by CHAYES (1975a,b, 1985). In these calculations the structural features and other properties will be calculated under the assumption that the whole rock analyses, as compiled in RKNFSYS, represent the bulk chemical composition of the igneous rocks in a completely molten state. It is recognized that this assumption does not take into account possible variations in $Fe^{3+}/\Sigma Fe$ during and subsequent to crystallization.

The rockfile RKNFSYS provides the opportunity to extract bulk compositional information based on rock names used in the original sources, on geographic distributions, age or by means of chemical discriminants. In the present report, calculations of structure of magmatic liquids will be done on large groups of analyses of commonly used names of extrusive igneous rocks. No attempt will be made to refine or redefine the names used in the original sources of the RKNFSYS, and the file will be employed with only one provision. It is considered unlikely that an unaltered extrusive igneous rock will contain more than 2 weight percent H_2O, and analyses with more than this amount of water have not been used. The range in concentration of each oxide together with the average value and standard error of these averages are shown in Table 1 together with the number of analyses in each group. This collection of analyses is by no means exhaustive, but it is hoped to be representative.

Structural information

The main features of silicate melt structure may be divided into four categories. These are (1) network-modifying cations (alkali metals, alkaline earths and ferrous iron), (2) aluminum and the relationship between tetrahedrally-coordinated Al^{3+} and cations required for electrical charge-balance of Al^{3+} in tetrahedral coordination, (3) ferric iron as a network-former (tetrahedrally-coordinated
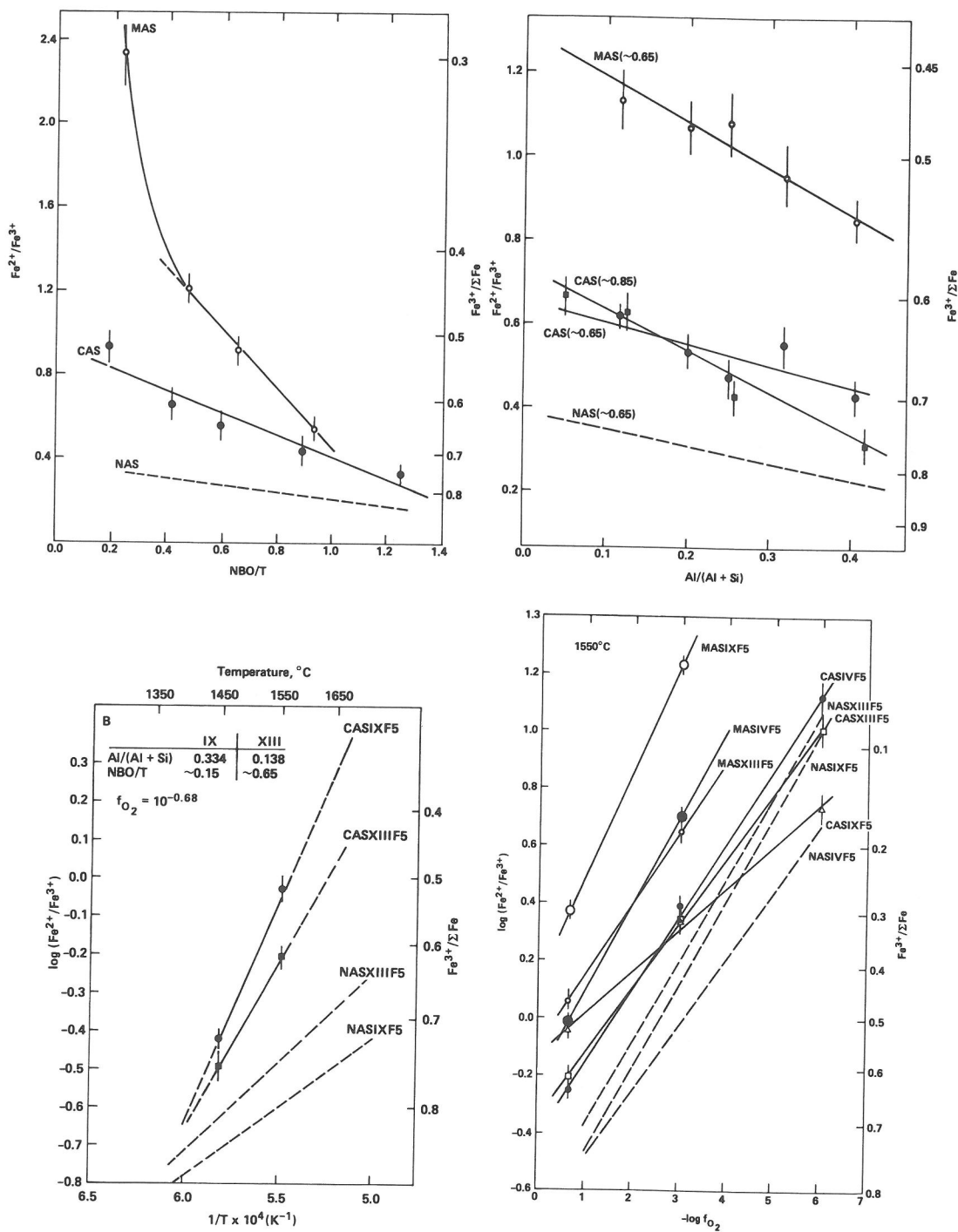
FIG. 2. Relations between $Fe^{3+}/\Sigma Fe$ and bulk melt $Al/(Al + Si)$, NBO/T (A), temperature (B) and oxygen fugacity (C). Abbreviations: NAS; system $Na_2O-Al_2O_3-SiO_2$, CAS; system $CaO-Al_2O_3-SiO_2$, MAS; system $MgO-Al_2O_3-SiO_2$. Roman numerals: IV, $Al/(Al + Si) = 0.334$ and NBO/T ~ 0.65; IX, $Al/(Al + Si) = 0.334$ and NBO/T ~ 0.15; XIII, $Al/(Al + Si) = 0.138$ and NBO/T ~ 0.65. For all compositions, 5 weight percent iron oxide was added as Fe_2O_3 (data from MYSEN et al., 1985b).

B. O. Mysen

Table 1. Bulk chemical information, common extrusive rocks

Name	Rhyolite			Dacite			Andesite		
No. of analyses	367			338			2068		
	Min.	Max.	Average	Min.	Max.	Average	Min.	Max.	Average
SiO_2	58.66	80.93	71.81 ± 3.44	50.79	79.20	65.23 ± 4.39	45.33	73.32	57.71 ± 4.19
Al_2O_3	7.97	19.10	13.65 ± 1.69	11.05	19.79	15.79 ± 1.50	10.95	23.71	17.25 ± 1.56
Fe_2O_3	0.00	7.17	1.89 ± 1.33	0.24	7.49	2.47 ± 1.24	0.00	12.16	3.09 ± 1.35
FeO	0.00	6.82	1.04 ± 1.05	0.00	8.16	2.56 ± 1.49	0.00	12.16	4.38 ± 1.77
MnO	0.00	0.31	0.06 ± 0.07	0.00	1.80	0.11 ± 0.17	0.00	1.91	0.14 ± 0.11
MgO	0.00	2.85	0.41 ± 0.43	0.08	5.97	1.75 ± 1.09	0.00	10.52	3.42 ± 1.40
CaO	0.00	6.31	1.33 ± 1.04	0.70	11.08	4.62 ± 1.80	0.11	12.37	7.09 ± 1.65
Na_2O	0.25	7.90	4.05 ± 1.18	1.83	7.56	3.76 ± 0.79	0.30	7.33	3.36 ± 0.78
K_2O	0.41	8.92	4.41 ± 1.19	0.28	8.06	2.08 ± 0.99	0.11	12.68	1.57 ± 0.82
TiO_2	0.00	1.20	0.30 ± 0.22	0.00	2.82	0.62 ± 0.32	0.00	5.10	0.88 ± 0.51
P_2O_5	0.00	0.94	0.07 ± 0.10	0.00	1.10	0.17 ± 0.12	0.00	2.32	0.23 ± 0.21

Name	Tholeiite & Olivine Tholeiite			Alkali Basalt			Basanite & Basanitoid		
No. of analyses	1010			279			206		
	Min.	Max.	Average	Min.	Max.	Average	Min.	Max.	Average
SiO_2	40.10	63.28	48.62 ± 2.94	35.69	58.20	46.33 ± 3.16	39.25	52.70	44.33 ± 2.55
Al_2O_3	3.62	24.05	15.10 ± 2.30	8.60	22.80	14.90 ± 2.03	8.31	19.53	14.40 ± 2.03
Fe_2O_3	0.04	11.91	3.46 ± 1.70	0.66	16.79	4.69 ± 2.24	0.91	10.50	4.44 ± 1.69
FeO	0.40	13.63	7.77 ± 1.79	0.39	10.94	7.12 ± 2.36	1.46	12.16	7.34 ± 2.13
MnO	0.00	1.23	0.17 ± 0.06	0.00	0.60	0.18 ± 0.07	0.00	1.48	0.17 ± 0.11
MgO	1.12	25.48	7.84 ± 2.79	2.04	20.17	8.09 ± 2.64	2.93	17.53	8.76 ± 2.79
CaO	4.36	15.12	10.17 ± 1.36	3.67	15.63	9.88 ± 1.73	5.89	15.50	10.58 ± 1.56
Na_2O	0.95	5.99	2.76 ± 0.69	1.18	7.73	3.20 ± 0.83	1.02	8.60	3.60 ± 1.03
K_2O	0.01	3.51	0.84 ± 0.55	0.16	3.09	1.28 ± 0.62	0.44	5.83	2.01 ± 1.08
TiO_2	0.00	6.50	2.00 ± 0.96	0.46	6.16	2.58 ± 0.96	0.42	5.86	2.59 ± 1.05
P_2O_5	0.00	1.71	0.35 ± 0.25	0.00	2.39	0.52 ± 0.33	0.00	1.99	0.62 ± 0.31

Name	Nephelinite		
No. of analyses	116		
	Min.	Max.	Average
SiO_2	35.68	44.75	39.95 ± 2.24
Al_2O_3	7.85	22.13	13.50 ± 2.78
Fe_2O_3	0.20	11.65	5.57 ± 2.15
FeO	0.54	11.05	6.76 ± 2.17
MnO	0.00	1.44	0.28 ± 0.22
MgO	1.03	19.45	7.86 ± 4.22
CaO	7.39	19.34	12.94 ± 2.21
Na_2O	1.26	14.24	4.54 ± 1.66
K_2O	0.54	9.00	3.32 ± 1.96
TiO_2	0.19	4.74	2.76 ± 0.75
P_2O_5	0.00	2.82	1.06 ± 0.51

Fe^{3+}) and network-modifier together with charge-balance considerations of tetrahedrally-coordinated Fe^{3+}, and (4) other cations (principally titanium and phosphorous). Experimental data from which all these aspects generally may be evaluated are available from a range of simple systems. As will be shown below, when such data do not exist, inter-polations and extrapolations may be conducted with some confidence.

(1) *Network-modifying cations.* From the frequencies, peak-heights and polarization behavior of appropriate Si-O stretch bands in Raman spectra of alkali metal-silica and alkaline earth-silica systems as a function of metal/silicon and type of metal

cation, BRAWER and WHITE (1975, 1977), VIRGO *et al.,* (1980), FURUKAWA *et al.,* (1981), MYSEN *et al.,* (1980b), MCMILLAN (1984), MATSON *et al.,* (1983) and VERWEIJ (1979a,b) concluded that the melt structures can be described in terms of a relatively small number of structural units. MYSEN *et al.,* (1982) extended the interpretations of these data by converting the Raman intensity data in the systems Na_2O-SiO_2, BaO-SiO_2, CaO-SiO_2 and $Ca_{0.5}Mg_{0.5}O$-SiO_2 to relative abundance of structural units in the melts. Those data are recast (Figure 3) as abundance of individual units as a function of Z/r^2 of the metal cation at fixed values of NBO/T

(NBO/T; nonbridging oxygen per tetrahedrally coordinated cations). The error bars in Figure 3 reflect the fitting errors for the Raman bands employed to calculate the relative abundance of the structural units. By progression of error calculations, the error in the abundance values typically is 10–15%. It is evident from those data that at a specific NBO/T value of the melt (corresponding to a specific metal/silicon), the abundance of TO_2 structural units (TO_2; three-dimensionally interconnected network) is positively correlated with Z/r^2 over the entire compositional range where TO_2 units could be detected. Because the overall polymerization of the
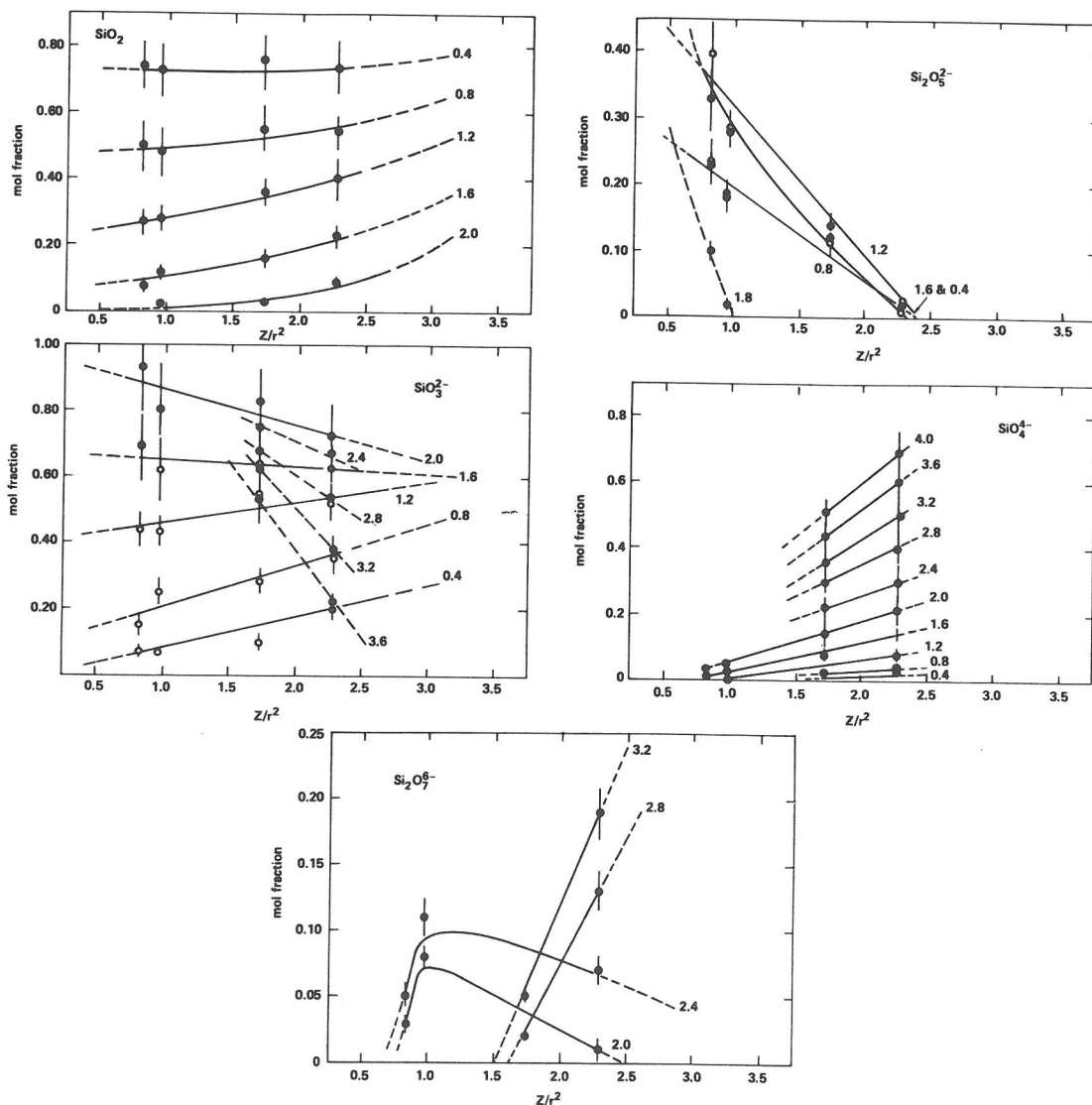
FIG. 3. Abundance of anionic structural units in binary metal oxide-silica systems as a function of Z/r^2 of the metal cation for bulk melt NBO/Si-values as indicated in the figure.

melts is not affected by the type of network-modifying metal cation, the abundance of depolymerized structural units in the melt (such units have NBO/T > 0) also varies with Z/r^2 (Figure 3). In the bulk melt NBO/T-range between 0 and about 2, the $X_{T_2O_5}$ decreases and the X_{TO_3} increases with increasing Z/r^2. For melt less polymerized than that of NBO/T ~ 2, T_2O_5 units generally are not detected, whereas X_{TO_3} and X_{TO_4} increase systematically with increasing Z/r^2 of the network-modifying cation.

By extrapolation of the curves in Figure 3 to $Z/r^2 = 0.47$ (potassium), 2.71 (ferrous iron) and 3.13 (magnesium), the abundance of anionic units in the systems K_2O-SiO_2, FeO-SiO_2 and MgO-SiO_2 is obtained. From this data base, the X_{TO_2}, $X_{T_2O_5}$, X_{TO_3}, $X_{T_2O_7}$ and X_{TO_4} can be expressed numerically (Table 2) as a function of bulk melt NBO/T for each major network-modifying cation in natural magmatic liquids (Figure 4). From these results (Figure 4), it is seen that the T_2O_5 units (NBO/T = 1) display decreasing abundance with increasing Z/r^2 so that for MgO-SiO_2, T_2O_5 units appear unstable and the proportion is quite small in the FeO-SiO_2 system. In those systems, TO_3 (NBO/T = 2) and TO_4 (NBO/T = 4) units are the principal depolymerized structural units. The maxima in T_2O_5 and TO_3 abundances occur near, but not necessarily at, the bulk melt NBO/T (or M/Si) corresponding to that degree of polymerization, a feature also observed by BRAWER and WHITE (1975, 1977) and FURUKAWA et al., (1981).

(2) *Aluminum.* Provided that large electropositive cations such as alkali metals or alkaline earths are available for electrical charge-balance, Al^{3+} is in tetrahedral coordination in silicate melts, at least at 1 bar pressure (*e.g.,* TAYLOR and BROWN, 1979a,b; NAVROTSKY et al., 1982, 1983; MCMILLAN et al., 1982; MYSEN et al., 1980b, 1982; SEIFERT et al., 1982; DOMINE and PIRIOU, 1986). Thus, melts on silica-aluminate joins have a three-dimensional network structure.

Substitution of Al^{3+} for Si^{4+} in tetrahedral coordination in crystalline materials results in a systematic decrease in T-O-T angle (BROWN et al., 1969; GIBBS et al., 1981) thus resulting in a lowering of the density of bonding electrons and, therefore, T-O bond strength. This decrease in bonding electron density is consistent with the 20% decrease in force constants for (Si,Al)-O stretching in the Al/(Al + Si)-range between 0 and 0.5 (SEIFERT et al., 1982; see also Figure 5) for melts on the join $NaAlO_2$-SiO_2.

Quantitative spectral data do not exist for melts on the join $KAlO_2$-SiO_2. Heat of mixing on joins such as $NaAlSi_2O_6$-$KAlSi_2O_6$ and $NaAlSi_4O_{10}$-

$KAlSi_4O_{10}$ (FRASER et al., 1983; FRASER and BOTTINGA, 1985) show only very subtle variations from 0 over most of the compositional range. It is, therefore, assumed that the structures of melt on the join $KAlO_2$-SiO_2 resemble those of melts on the join $NaAlO_2$-SiO_2. As a result, in the present discussion, K^+ and Na^+ as charge-balancing cations for Al^{3+} are treated similarly.

There is, however, a pronounced difference between the structural interpretation of vibrational spectra of melts on the join $NaAlO_2$-SiO_2 and those on the joins $CaAl_2O_4$-SiO_2 and $MgAl_2O_4$-SiO_2, where the spectra indicate significant (Si,Al)-ordering (SEIFERT et al., 1982; MCMILLAN et al., 1982; see also NAVROTSKY et al., 1982; RICHET and BOTTINGA, 1985, 1986; for detailed discussion on relationships between thermodynamic and structural data).

A detailed and quantitative model was suggested by SEIFERT et al., (1982), who from Raman spectroscopic data found that these latter melts could be described in terms of mixing of a small number of three-dimensionally interconnected structural units. Their proportions, but not their Al/(Al + Si), vary as systematic functions of the bulk melt Al/(Al + Si) (Figure 6). There are small, and perhaps insignificant, differences between the structure of melts on the joins $CaAl_2O_4$-SiO_2 and $MgAl_2O_4$-SiO_2. Coefficients from least-squares fitted curves through these data are provided in Table 3.

With compositions of melts on $MAlO_2$-$M''Al_2O_4$-SiO_2 joins (M; monovalent cation, M''; divalent cation), it is considered, therefore, that the melts can be described in terms of $(Al,Si)_3O_8^-$, $Al_2Si_2O_8^{2-}$ and AlO_2^- units. For a specific Al/(Al + Si), the abundance of these three-dimensionally-interconnected units does vary, therefore, with M/M''. An example is shown in Figure 7 for melts on the join $NaAlSi_3O_8$-$CaAl_2Si_2O_8$. For all but the melts near the anorthite composition, these can be described in terms of two three-dimensional network structural units. One is of the type $Al_2Si_2O_8^{2-}$ with, therefore, constant Al/(Al + Si) across the entire composition join. The other unit, $(Al,Si)_3O_8^-$, exhibits a slowly decreasing Al/(Al + Si) as the proportion of anorthite component in the melt increases.

It has been observed (*e.g.,* BROWN et al., 1969) that in structures of crystalline aluminosilicates with a range of T-O-T angles, Al^{3+} exhibits a preference for the sites associated with the smallest T-O-T angle. In silicate melts with bulk melt NBO/T > 0, structural units with different T-O-T angles coexist (FURUKAWA et al., 1981; VIRGO et al., 1980). In general, the greater the NBO/T of an individual unit in a melt, the larger the T-O-T (FURUKAWA

Table 2. Regression coefficients,* mol fraction of structural units

TO_2

Network-modifier	a	b	c	d	e
K	1.01 ± 0.03	-0.83 ± 0.06	0.16 ± 0.03		
Na	1.01 ± 0.02	-0.76 ± 0.05	0.12 ± 0.03		
Ca	1.00 ± 0.02	-0.76 ± 0.02	0.13 ± 0.01		
Fe^{2+}	0.99 ± 0.02	-0.60 ± 0.05	0.05 ± 0.02		
Mg	0.98 ± 0.03	-0.47 ± 0.07	0.05 ± 0.02		

T_2O_5

Network-modifier	a	b	c	d	e
K	-0.07 ± 0.03	1.18 ± 0.09	-0.60 ± 0.05		
Na	-0.04 ± 0.01	0.91 ± 0.04	-0.39 ± 0.06	-0.17 ± 0.03	0.08 ± 0.01
Ca	0.06 ± 0.02	0.17 ± 0.14	-0.09 ± 0.02		
Fe^{2+}		Not stable			
Mg			Not stable		

TO_3

Network-modifier	a	b	c	d	e
K	-0.26 ± 0.06	0.58 ± 0.04			
Na	-0.22 ± 0.07	0.57 ± 0.05			
Ca	-0.03 ± 0.01	0.17 ± 0.03	0.32 ± 0.04	-0.10 ± 0.02	-0.001 ± 0.001
Fe^{2+}	-0.08 ± 0.03	0.87 ± 0.09	-0.29 ± 0.06	0.01 ± 0.01	
Mg	-0.05 ± 0.01	0.86 ± 0.06	-0.26 ± 0.02		

T_2O_7

Network-modifier	a	b	c	d	e
K			No data available		
Na			No data available		
Ca	-0.120 ± 0.001	0.500 ± 0.001			
Fe^{2+}	-0.55 ± 0.09	0.27 ± 0.04			
Mg	-0.7 ± 0.1	0.35 ± 0.07			

TO_4

Network-modifier	a	b	c	d	e
K			No data available		
Na	0.2 ± 0.1	-0.3 ± 0.1	0.09 ± 0.04		
Ca	0.023 ± 0.001	-0.032 ± 0.003	0.049 ± 0.002	-0.001 ± 0.001	
Fe^{2+}	-0.03 ± 0.01	0.09 ± 0.02	0.035 ± 0.004		
Mg	-0.04 ± 0.02	0.11 ± 0.03	0.039 ± 0.006		

* Expression: $X = a + b(NBO/T) + c(NBO/T)^2 + d(NBO/T)^3 + e(NBO/T)^4$.

et al., 1981). This logic leads to the suggestion that aluminum should exhibit a preference for the most polymerized structural unit in the melts, a suggestion that is supported by observation (MYSEN *et al.,* 1981a, 1985a; DOMINE and PIRIOU, 1986). For aluminosilicate melts with Al_2O_3 concentrations in the range observed in natural magmatic liquids (see Table 1), the ratio $[Al/(Al + Si)]^{TO_2}/[Al/(Al + Si)]^{T_2O_5}$ is near 2 and that of $[Al/(Al + Si)]^{T_2O_5}/[Al/(Al + Si)]^{TO_3}$ near 1.5 (MYSEN *et al.,*
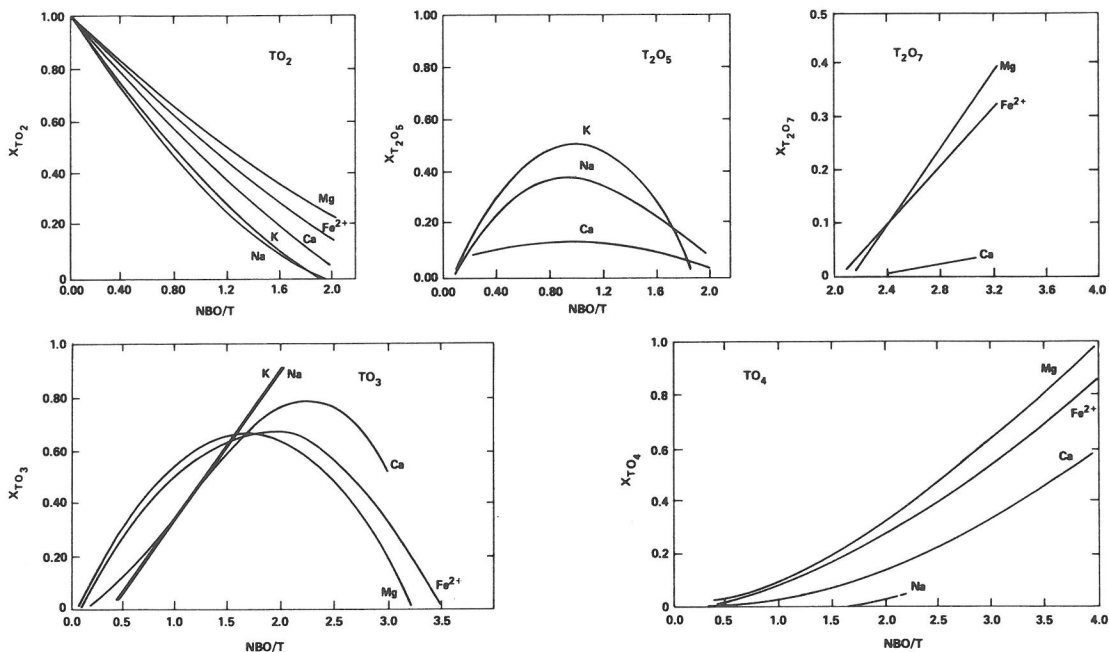
FIG. 4. Calculated abundance curves of anionic structural units in the systems $K_2O\text{-}SiO_2$, $Na_2O\text{-}SiO_2$, $CaO\text{-}SiO_2$, $FeO\text{-}SiO_2$ and $MgO\text{-}SiO_2$.

1981a). These values are not completely independent of bulk composition (changes in charge-balancing cations and degree of melt polymerization) and probably temperature and pressure (MYSEN *et al.*, 1985a). Available experimental data do not, however, permit a detailed assessment of these

variables. For the present discussion the values of 2.0 and 1.5 will be used.

In natural magmatic liquids, cations such as K^+, Na^+, Ca^{2+}, Mg^{2+} and Fe^{2+} are major components. All or portions of these may occur as charge-balancing cations for Al^{3+} in tetrahedral coordination. Thermodynamic data from glasses and melts on silica-aluminate joins (NAVROTSKY *et al.*, 1980,
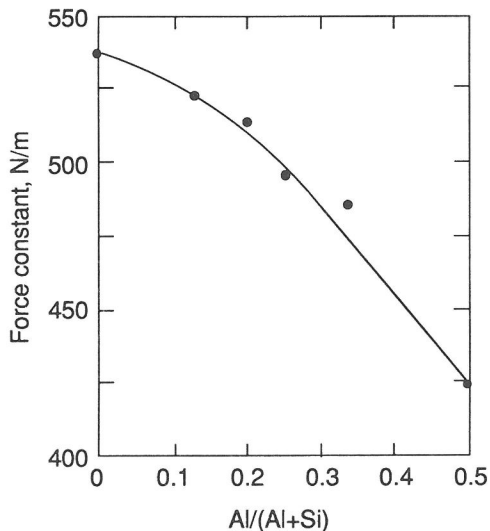
FIG. 5. Force constants for $(Si,Al)\text{-}O^0$ stretch vibrations as a function of bulk melt $Al/(Al + Si)$ along the join $SiO_2\text{-}NaAlO_2$ (data from SEIFERT *et al.*, 1982).
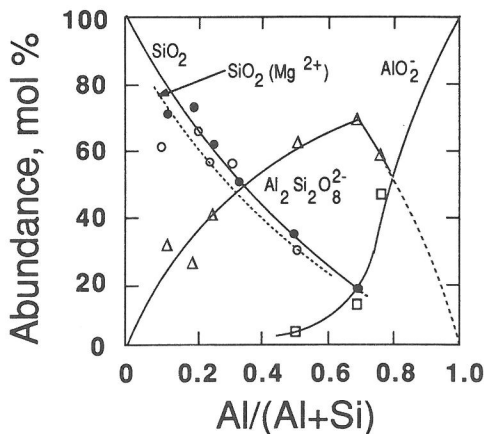
FIG. 6. Abundance of three-dimensionally-interconnected structural units in the systems $SiO_2\text{-}CaAl_2O_4$ and $SiO_2\text{-}MgAl_2O_4$ as a function of $Al/(Al + Si)$ (data from SEIFERT *et al.*, 1982).

Table 3. Regression coefficients,* aluminate structural units

Unit type	a	b	c	d	e
$(Al, Si)_3O_8^-$	0.93 ± 0.04	-1.5 ± 0.2	0.6 ± 0.2		
$Al_2Si_2O_8^{2-}$	0.012 ± 0.005	2.2 ± 0.8	-3.8 ± 0.4	5.6 ± 0.6	-3.9 ± 0.3
AlO_2^{2-}	0.4 ± 0.2	-2.1 ± 0.7	2.7 ± 0.5		

* Expression: $X = a + b[Al/(Al + Si)] + c[Al/(Al + Si)]^2 + d[Al/(Al + Si)]^3 + e[Al/(Al + Si)]^4$.

1982, 1983; RAY and NAVROTSKY, 1984) can be used to establish a hierarchy of relative stabilities of aluminum-bearing silicate units in the melts. Heat of solution data show that the relative stabilities are positively correlated with Z/r^2 of the charge-balancing cation (Figure 8), a suggestion first made by BOTTINGA and WEILL (1972). Thus, the hierarchy of stabilities are $K^+ > Na^+ > Ca^{2+} > Mg^{2+}$. Because the Z/r^2 of Fe^{2+} is between that of Ca^{2+} and Mg^{2+}, it is likely that Fe^{2+}-charge-balanced aluminate complexes are less stable than those of Ca^{2+}, but more so than those of Mg^{2+}.

(3) *Ferric iron.* Iron oxides in magmatic liquids is of interest in part because redox relations may be employed to deduce pressure-temperature-oxygen fugacity relations (*e.g.,* KENNEDY, 1948; FUDALI, 1965; MO *et al.,* 1982; SACK *et al.,* 1980; KILINC *et al.,* 1983; VIRGO and MYSEN, 1985; MYSEN, 1986). The principal relationships may be illustrated with the expression (MO *et al.,* 1982):

$$\ln f_{O_2}^{P} = \ln f_{O_2}^{1 \, bar} + \frac{(2\overline{V}_{Fe_2O_3} - 4\overline{V}_{FeO})(P-1)}{RT}. \quad (1)$$

The temperature-dependence of the redox ratio can be inferred from the RT-term and a possible pressure dependence from the volume term, where experimental data (MO *et al.,* 1982; BOTTINGA *et al.,* 1983) show that at least at 1 bar pressure, the partial molar volume of ferric oxide exceeds that of ferrous oxide in silicate melts. Thus, at constant oxygen fugacity, composition and temperature, the ferric/ferrous of a melt should decrease with increasing pressure. This suggestion has been experimentally verified (MYSEN and VIRGO, 1978, 1985).

Ferric and ferrous oxide in magmatic liquids are additionally important because a change in redox ratio affects the structure of the melt, and, therefore, melt properties that are governed by its structure (*e.g.,* MYSEN and VIRGO, 1980; MYSEN *et al.,* 1984, 1985c; FOX *et al.,* 1982; DICKENSON and HESS, 1981, 1986). Structural data for iron-bearing melts have been reported mostly for binary metal oxide-silica and ternary metal oxide-alumina-silica melts. Evidence from optical and luminescence spectroscopy (FOX *et al.,* 1982), optical spectroscopy (NOLET *et al.,* 1979) Raman and Mossbauer spectroscopy (*e.g.,* FOX *et al.,* 1982; MYSEN *et al.,* 1980b,

FIG. 7. Calculated abundance of structural units in melts on the join $NaAlSi_3O_8$-$CaAl_2Si_2O_8$.
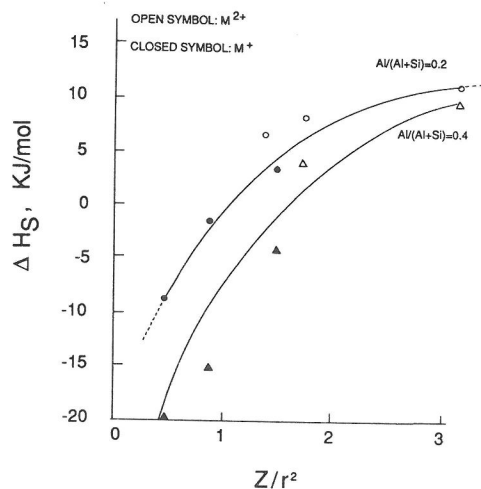
FIG. 8. Heat of solution of quenched melts along aluminate-silica join as a function of Z/r^2 of the charge-balancing cation (heat of solution data from NAVROTSKY *et al.,* 1980, 1982, 1983; RAY and NAVROTSKY, 1984).
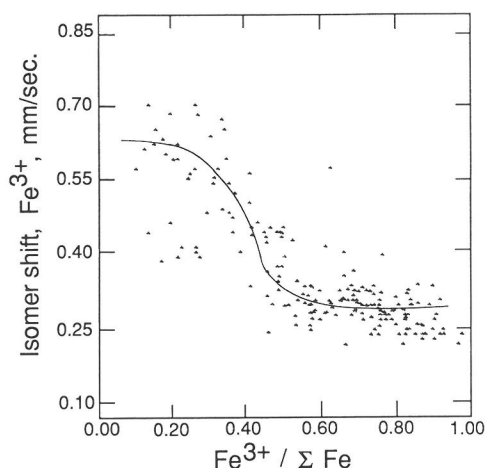
FIG. 9. Isomer shifts of ferric iron relative to that of iron metal ($IS_{Fe^{3+}}$, mm/sec) as a function of $Fe^{3+}/\Sigma Fe$ for quenched melts in the systems $CaO-SiO_2$, $(Ca_{0.5}Mg_{0.5})O-SiO_2$, Na_2O-SiO_2, $CaO-Al_2O_3-SiO_2$ and $MgO-Al_2O_3-SiO_2$ with total iron contents in the range 5 to 15 weight percent (as Fe_2O_3) (data from MYSEN et al., 1984, 1985b,c; MYSEN and VIRGO, 1985).

1984, 1985b; SEIFERT et al., 1979; VIRGO and MYSEN, 1985) and electron spin resonance spectroscopy (CALAS and PETIAU, 1983) indicate that whereas ferrous iron is a network-modifier in the temperature, oxygen fugacity and compositional ranges of igneous processes, ferric iron may play a dual role. From Mossbauer spectroscopy, the isomer shift of Fe^{3+} ($IS_{Fe^{3+}}$) is a sensitive indicator of the oxygen polyhedron around Fe^{3+}. For values (relative to Fe metal) greater than about 0.5 mm/sec, Fe^{3+} is a network-modifier, whereas with $IS_{Fe^{3+}} < 0.3$ mm/sec, Fe^{3+} is a network-former (VIRGO and MYSEN, 1985). In the range between 0.3 and 0.5 mm/sec, both network-forming and network-modifying Fe^{3+} coexist (see VIRGO and MYSEN, 1985, for a detailed review of the evidence). On the basis

of several hundred Mossbauer analyses of quenched melts at 1 bar and at high pressure, it appears, therefore, that the $Fe^{3+}/\Sigma Fe$ of the melts is closely related to the structural position of Fe^{3+} (Figure 9). From the compilation of chemical analyses of cenozoic volcanic rocks (CHAYES, 1975a,b, 1985), one may derive information for the structural role of Fe^{3+} in their molten state provided that the published bulk chemical $Fe^{3+}/\Sigma Fe$ values represent the redox ratio of iron in these rocks prior to crystallization (Table 4). Most likely ferric iron occurs as both a network-former and as network-modifier in natural magmatic liquids. It is also evident from those data that the proportion of tetrahedrally-coordinated ferric iron becomes increasingly important the more felsic the magmatic liquid (more polymerized the liquid) although one may suggest that increasing alkalinity also results in more tetrahedrally-coordinated ferric iron. These generalizations have been quantified in binary and ternary systems used in laboratory studies, where a clear relationship between $Al/(Al + Si)$ (Figure 2) and type metal cations have been observed (Figure 10). Increasing $Al/(Al + Si)$ and decreasing Z/r^2 of the metal cations result in enhanced $Fe^{3+}/\Sigma Fe$.

Qualitatively, the behavior of tetrahedrally-coordinated ferric iron resembles that of Al^{3+} in that it requires electrical charge-balance with alkali metals, alkaline earths or ferrous iron. VIRGO and MYSEN (1985) in a summary of spectroscopic data relevant to iron oxides in silicate melts concluded, however, that in contrast to Al^{3+}, regardless of the type of charge-balancing cation, random substitution of Fe^{3+} for Si^{4+} in melt structural units does not appear to take place. Rather, ferrisilicate or ferrite structural units with constant $Fe^{3+}/(Fe^{3+} + Si)$ are stabilized, and the proportions of such units may be functions of bulk melt $Fe^{3+}/(Fe^{3+} + Si)$. Additional structural information similar to that of aluminum is not yet available. In the present report,

Table 4. Percent of rock analyses within $Fe^{3+}/\Sigma Fe$ brackets indicated

Name	Rhyolite	Dacite	Andesite	Tholeiite & Olivine Tholeiite	Alkali Basalt	Basanite & Basanitoid	Nephelinite
No. analyses	367	338	2068	1010	279	206	116
$Fe^{3+}/\Sigma Fe$	0.63 ± 0.25	0.48 ± 0.20	0.40 ± 0.07	0.29 ± 0.13	0.38 ± 0.19	0.36 ± 0.14	0.43 ± 0.16
$<0.3^*$	13.9	23.3	28.9	58.3	63.4	62.6	23.3
0.3–0.5†	17.2	43.1	49.7	34.7	40.1	46.2	43.1
>0.5‡	68.9	33.6	21.5	7.0	23.3	16.5	33.6

* With $Fe^{3+}/\Sigma Fe < 0.3$, all Fe^{3+} in melt is network-modifier.
† With $Fe^{3+}/\Sigma Fe = 0.3-0.5$, Fe^{3+} in melt is partially network-modifier and partially network-former.
‡ With $Fe^{3+}/\Sigma Fe > 0.5$, all Fe^{3+} in melt is network-former.
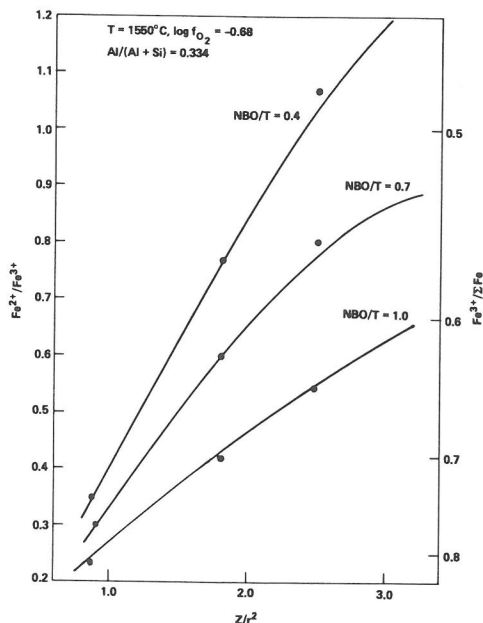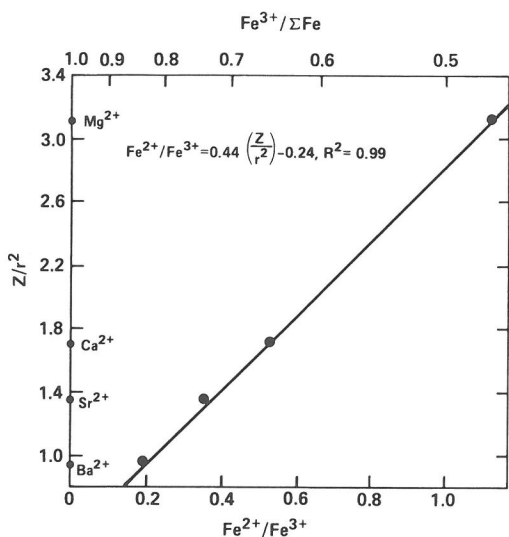
FIG. 10. $Fe^{3+}/\Sigma Fe$ as a function of Z/r^2 of metal cation in metal oxide-silica and metal oxide-alumina-silica systems as indicated on figure (data from MYSEN *et al.*, 1984, 1985b).

tetrahedrally coordinated ferric iron will be considered as a separate unit with no additional breakdown. It is suggested, however, that a hierarchy in relative stability exists. In contrast with the silica-alumina systems (Figure 8), not enough data are available for relative stabilities of ferric iron complexes. In view of the many similarities in structural behavior of tetrahedrally-coordinated ferric iron and aluminum, it is suggested that a hierarchy similar to that of aluminum charge-balance exists for tetrahedrally-coordinated ferric iron (*i.e.*, K > Na > Ca > Fe^{2+} > Mg).

(4) *Other cations.* Among the major element oxides in igneous rocks, titanium and phosphorous generally are the least abundant (Table 1). Nevertheless, these two oxides have attracted considerable attention because even in their natural concentration ranges melt properties are profoundly affected (*e.g.*, KUSHIRO, 1975; VISSER and VAN GROOS, 1979; WATSON, 1976; RYERSON and HESS, 1980; DICKINSON and HESS, 1985). Both Ti^{4+} and P^{5+} enhances the activity coefficients of SiO_2 in silicate melts. (KUSHIRO, 1975; RYERSON, 1985) in contrast to components such as alkali metals or alkaline earths. Thus, it has been frequently suggested (*e.g.*, KUSHIRO, 1975; WATSON, 1976; RYERSON and HESS, 1980; VISSER and VAN GROOS, 1979) that both cations act as network-formers in silicate melts.

Vibrational spectroscopic data of phosphorous-bearing melts support this conclusion (*e.g.*, GALEENER and MIKKELSEN, 1979; NELSON and EXHAROS, 1979; MYSEN *et al.*, 1981b; NELSON and TALLANT, 1984). Those data also indicate that in depolymerized melts (NBO/T > 0), phosphorous occurs in phosphate complexes either in the form of PO_3^- (NELSON and EXHAROS, 1979; MYSEN *et al.*, 1981b) or as PO_4^{3-} complexes (NELSON and TALLANT, 1984). These complexes are electrically neutralized with alkali metals or alkaline earths. Although it has not been established which cation or cations are involved in this process, free energy of formation data for crystalline analogues indicate that calcium phosphate complexing is the most likely.

The vibrational data for titanium-bearing silicate melts are less conclusive than those for phosphorous-bearing systems. TOBIN and BAAK (1968) investigated the system SiO_2-TiO_2 and suggested that titanium is in four-fold coordination and CHANDRASEKHAR *et al.*, (1979) implied that the structure of vitreous TiO_2 resembles that of vitreous SiO_2 (three-dimensionally-interconnected network). X-ray absorption data on SiO_2-TiO_2 glasses (*e.g.*, SANDSTROM *et al.*, 1980) indicate that both tetrahedral and octahedral Ti^{4+} may occur, and that tetrahedral coordination becomes more dominant with increasing Ti-content. FURUKAWA and WHITE

(1979), in their study of glass structure in the system $Li_2Si_2O_5$-TiO_2 suggested that at least some of the Ti^{4+} might not occur in tetrahedral coordination. MYSEN *et al.,* (1980c) observed that the frequency of Raman bands from Si-O⁻ stretching decreasing somewhat as a function of increasing bulk melt Ti/ (Ti + Si). They also observed that Ca- and Ca,Mg-metasilicate melts became more polymerized as TiO_2 was added. These observations suggest that Ti^{4+} may be tetrahedrally-coordinated in the melts. It was also observed, however, that vibrational spectra of crystals and quenched melts of Na_2TiO_3 composition exhibited significant similarities. Similar comparisons were conducted in the system K_2O-TiO_2 by DICKINSON and HESS (1985). The latter authors suggested that in the silica-free titanate systems, titanium occurs principally in a highly distorted octahedron. The data by MYSEN *et al.,* (1980c) for Na_2O-TiO_2 could be interpreted similarly. From these, seemingly somewhat conflicting, data it would appear that most likely titanium occurs in more than one coordination state in silicate melts. The exact compositional control on the proportions of the individual coordination polyhedra as well as the type of coordination polyhedra remains open to further investigation.

STRUCTURE OF MAGMATIC LIQUIDS

The structural data detailed above can be combined to describe the structure of magmatic liquids on the basis of their bulk chemical composition. The first step in this procedure is to establish the proportions of tetrahedrally-coordinated cations and the types and proportions of cations required for electrical charge-balance. Phosphorous most likely occurs as orthophosphate (PO_4^{3-}) and are considered in association with Ca^{2+}. Thus, for each P^{5+} cation, 1.5 Ca^{2+} is required. This proportion of Ca^{2+} is, therefore, subtracted from the total amount present. The proportion of ferric iron in tetrahedral coordination is calculated on the basis of $Fe^{3+}/\Sigma Fe$ as indicated above (see also Figure 9). Both Al^{3+} and Fe^{3+} require charge-balance in tetrahedral coordination and the hierarchy of relative stabilities of the Al^{3+}- and Fe^{3+}-complexes is identical. The ferric iron is assigned first. Thus, for potassium, for example, if there is sufficient amount available, a proportion equivalent to the proportion of Fe^{3+} is assigned and this proportion is subtracted from the total potassium concentration before assignment of the remainder (and possibly other cations) as charge-balancing cations for Al^{3+}. If there is insufficient potassium in the melt, the sodium is also a charge-balancing cation for tetrahedrally-coordinated Fe^{3+}. In that case, no potassium can charge-balance Al^{3+}. The complete procedure is carried out in the order

K^+, Na^+, Ca^{2+}, Mg^{2+} first with assignment to Fe^{3+} and then to Al^{3+}. The bulk melt NBO/T of a natural magmatic liquid now can be calculated from the expression:

$$NBO/T = 1/T \sum_{i=1}^{i} M_i^{n+}, \qquad (2)$$

where M_i^{n+} is the proportion of network-modifying cation i with electrical charge n^+ and T is the proportion of tetrahedrally coordinated cations.

Distribution of NBO/T of melts of rhyolite, andesite, tholeiite and basanite melt compositions is shown in Figure 11. It is evident from those data that most common extrusive igneous rocks have NBO/T-values between 0 and 1 and that the more felsic the igneous rock, the more polymerized it is. There are distinct maxima in the NBO/T distributions for each rock type, but the range of values spread quite widely in particular for the basanite composition as also reflected in the standard errors of the average NBO/T calculated for seven major igneous rock types (Table 5).

As a result of the charge-balancing requirements for Al^{3+} and Fe^{3+} in tetrahedral coordination, metal cations that exist as network-modifiers in simple metal oxide-silica systems, may not always be network-modifiers in natural magmatic liquids (Table 5). For example, the alkali metal contents of most igneous extrusive rocks generally are so low that only in a fraction of the rhyolite and nephelinite compositions will Na or K occur as network-mod-
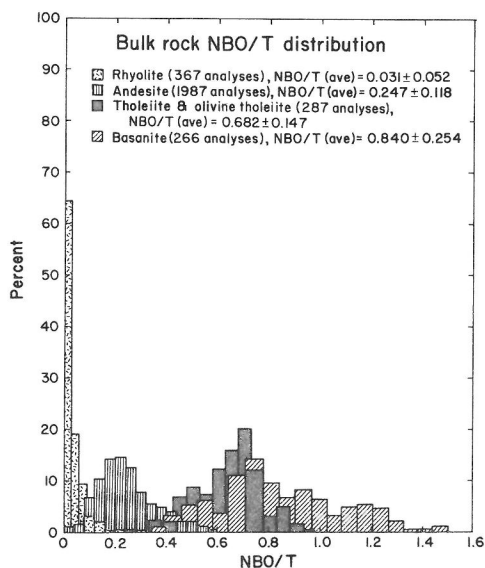
FIG. 11. Distribution of bulk melt NBO/T of magmatic liquids as indicated on figure. The rock analyses were extracted from rockfile RKNFSYS (CHAYES, 1975a,b; 1985; see also discussion in text).

Table 5. Percentage of analyses where individual metal cations are network-modifiers

Name	Rhyolite	Dacite	Andesite	Tholeiite & Olivine Tholeiite	Alkali Basalt	Basanite & Basanitoid	Nephelinite
No. analyses	367	338	2068	1010	279	206	116
Na + K	5.5	0.0	0.0	0.01	0.0	0.0	4.3
Ca	22.9	31.1	61.4	98.3	92.8	100.0	100.0
Fe^{2+}	50.4	79.3	94.9	100.0	100.0	100.0	100.0
Mg	99.2	00.4	99.9	100.0	100.0	100.0	100.0
Fe^{3+} *	100.0	100.0	100.0	100.0	100.0	100.0	100.0

* Where $Fe^{3+}/\Sigma Fe$ is sufficiently low so that some or all Fe^{3+} is network-modifier.

ifiers. In all other compositions, and in most rhyolites and nephelinites, $[(Al^{3+}(IV) + Fe^{3+}(IV)] > [Na + K]$ and all alkali metals are charge-balancing cations. In fact, for a given rock type, the more electronegative the metal cation, the larger is the proportion of melts where the metal cation occurs as a network-modifier. For a given metal cation, the more polymerized the melt (the smaller the bulk melt NBO/T), the smaller the fraction of analyses where this cation occurs as a network-modifier (Table 5).

Fractions of nonbridging oxygens in magmatic liquids associated with individual network-modifying cations are shown in Figure 12. It can be seen from those data that ferrous iron and magnesium are the most important network-modifying cations in melts of common extrusive igneous rocks. In all but the most felsic rocks (rhyolite), magnesium is the most important followed by ferrous iron. In rhyolite composition melts, the relative importance of ferrous iron and magnesium is reversed. The data in Figure 12 also illustrate the fact that Na + K is relatively unimportant as network-modifier in natural magmatic liquids.

The abundance of anionic structural units in natural magmatic liquids can be estimated with the aid of the expressions in Table 2. In order to employ those equations for complex natural melts, the mol fraction of a structural unit associated with a particular network-modifying cation must be multiplied by the atomic proportion of the network-modifying cation in question. For example, if $X_{TO_3}^{Mg}$ from Table 2 is 0.5 and the atomic fraction of the network-modifying cation is 0.25, the fraction of TO_3 associated with Mg^{2+} in the melt is 0.125. The overall abundance of each structural unit is then given by the summations:

$$X_{T_2O_5} = \sum_{i=1}^{i} T_2O_{5i}, \tag{3}$$

$$X_{TO_3} = \sum_{i=1}^{i} TO_{3i}, \tag{4}$$

$$X_{T_2O_7} = \sum_{i=1}^{i} T_2O_{7i}, \tag{5}$$

$$X_{TO_4} = \sum_{i=1}^{i} TO_{4i} \tag{6}$$

and

$$X_{TO_2} = 1.0 - (X_{T_2O_5} + X_{TO_3} + X_{T_2O_7} + X_{TO_4}), \tag{7}$$

where T_2O_{5i} etc. is the proportion of specified structural unit associated with network-modifying cat-
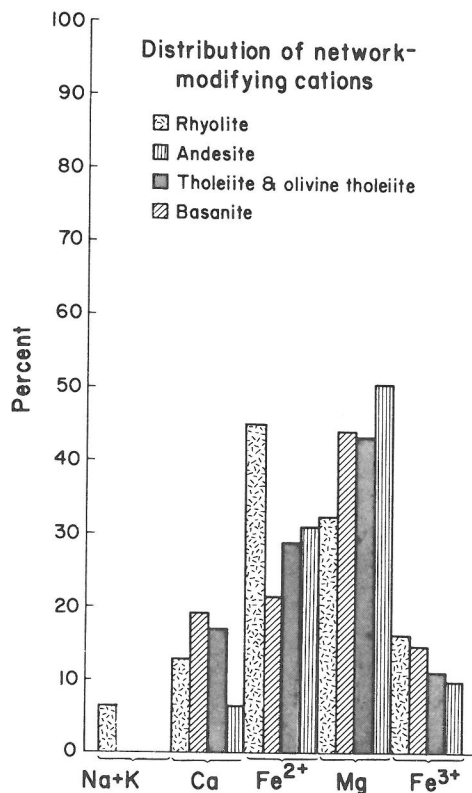
FIG. 12. Distribution of network-modifying cations in melts major extrusive rock types. (CHAYES, 1975a,b; 1985; see also discussion in text).

ion, *i*, and $X_{T_2O_5}$ etc. represent the total abundance of this structural unit in the melt.

The distribution of structural units in a subset of rhyolite, andesite, tholeiite and basanite (2295 analyses in total) as a function of bulk melt NBO/T is shown in Figure 13. The distribution of $X_{T_2O_7}$ is not shown because only 20 of the 2295 analyses show any amount of $X_{T_2O_7}$, and even in those cases this amount was vanishingly small. One may conclude, therefore, that pyrosilicate structural units are uncommon in melts of common extrusive igneous rocks. The distribution of T_2O_5 exhibits a distinct maximum at bulk melt NBO/T near 0.5. This NBO/T-value corresponds to quartz tholeiite and basaltic andesite. The results (Figure 13) illustrate that TO_2 and TO_3 are the most common structural units in most natural magmatic liquids with the possible exception of compositions in the NBO/T-range between 0.3 and 0.4 (typically corresponding to andesite), where T_2O_5 units may be more important and for compositions with bulk NBO/T < 0.2 (corresponding to rhyolite and the most felsic andesite compositions), where TO_3 units are not present in the melt and the nonbridging oxygens occur only in TO_4 and T_2O_5 units. This structure distribution results from the fact that alkalies and Ca^{2+} are associated with T_2O_5 units in these rock types (Figure 14), whereas magnesium, and to a lesser degree, ferrous iron, exhibits a pronounced preference for TO_4 units.
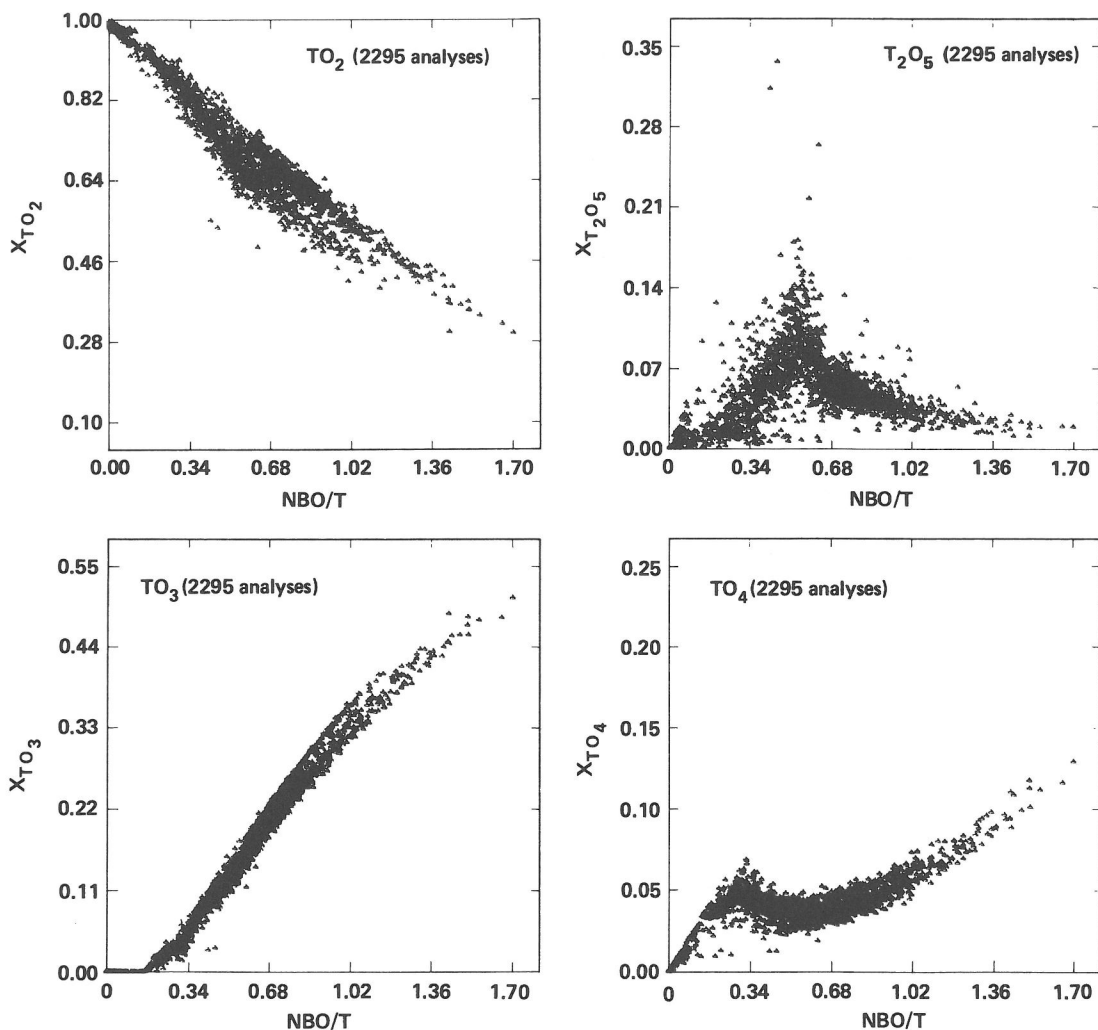
FIG. 13. Distribution of individual anionic structural units in major rock types as a function of bulk melt NBO/T. Rock analyses were extracted from rockfile RKNFSYS (CHAYES, 1975a,b; 1985; see also discussion in text).
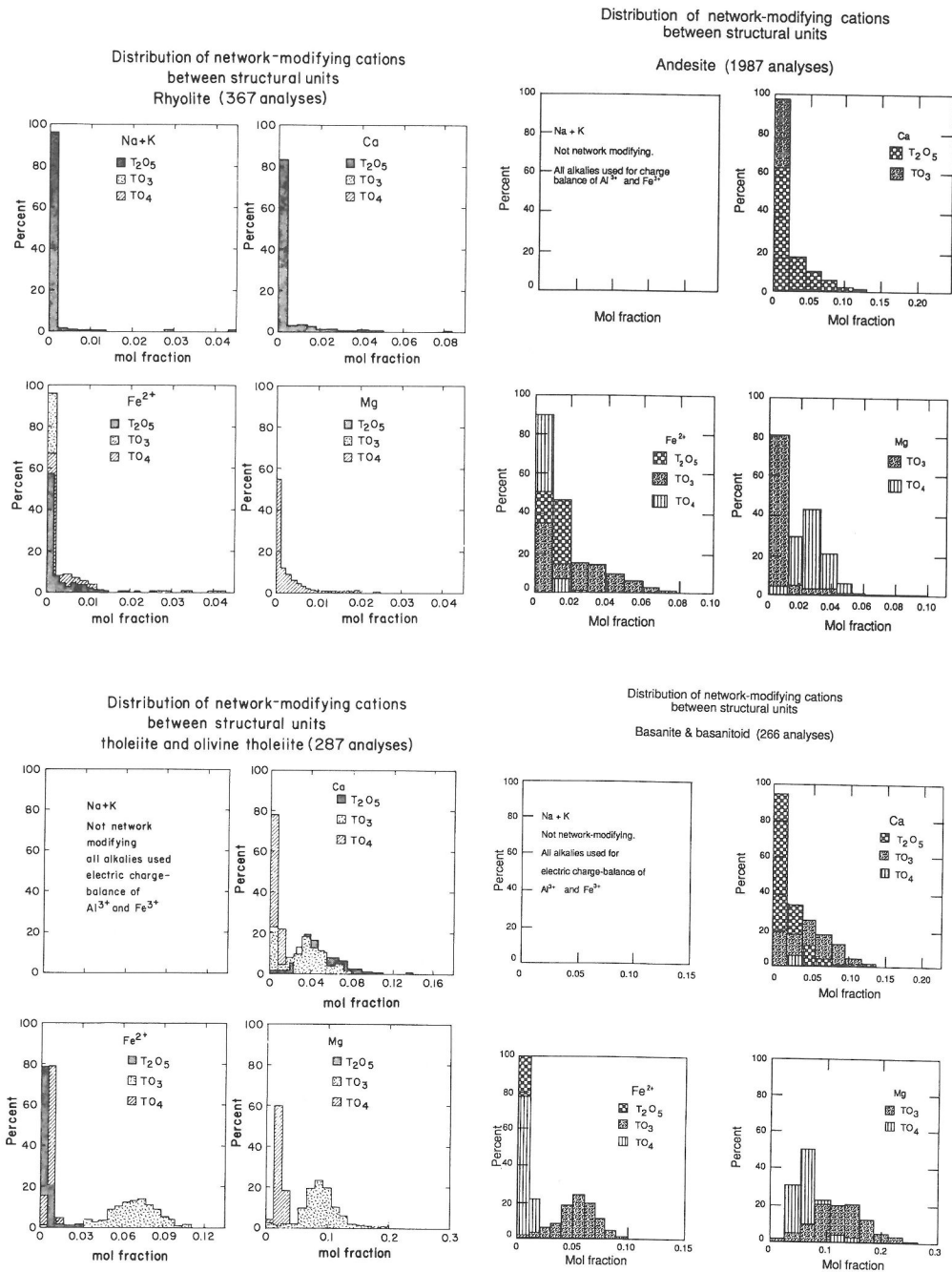
FIG. 14. Network-modifying cation distribution among individual anionic structural units in melts of major extrusive rock types. (A) Rhyolite, (B) Andesite, (C) Tholeiite and olivine tholeiite and (D) Basanite and basanitoid (CHAYES, 1975a,b; 1985; see also discussion in text).

The abundance of three-dimensional network units was obtained by mass balance [equation (8)]. With the exception of a few basanite analyses, these TO_2 units can be described as a mixture of alkali charge-balanced $AlSi_3O_8^-$ and predominantly alkaline earth balanced $Al_2Si_2O_8^{2-}$. For andesitic and more felsic rocks, a significant proportion of the Al^{3+} is also charge-balanced with ferrous iron as the

summary in Table 5 indicates that for these rocks only ~20–50% of these compositions have insufficient Ca^{2+} for aluminum electrical charge-balance.

PETROLOGICAL APPLICATIONS

Structure and properties of magmatic liquids

Recent experimental data indicate that partial molar volumes of the major element oxides in magmatic liquids are independent of bulk chemical composition in the compositional range between rhyolite and basalt (MO *et al.,* 1982; BOTTINGA *et al.,* 1983). From the partial molar volume data, the molar volume of a magmatic liquid is calculated from the expression:

$$V = \sum_{i=1}^{i} X_i \overline{V}_i, \qquad (9)$$

where $\overline{V}_i$ and X_i are the partial molar volume and mol fraction of oxide component *i*. The distribution of molar volumes calculated from 2607 rock analyses from RKNFSYS is shown in Figure 15. This histogram exhibits a slightly skewed distribution

where the enrichment near 28 cm³/mol reflects the rhyolite analyses (average: 28.3 ± 0.4 cm³/mol). The maximum near 26 cm³/mol represents a mixture of the remaining rock types (average values are: basanite, 23.8 ± 0.9 cm³/mol; tholeiite, 24.0 ± 0.5 cm³/mol; andesite, 26.3 ± 0.7 cm³/mol) although there is a general positive correlation between molar volume and degree of polymerization of the melt (Figure 16). A very simple positive linear correlation exists, however, between the proportion of three-dimensional network units in the melt (Figure 16) with the least-squares fitted straight line:

$$V = 16.33 \pm 0.05 + 11.72 \pm 0.07 X_{TO_2}. \quad (10)$$

As shown above (Figure 13), the proportions of TO_3 and TO_4 units vary inversely with TO_2. Thus, as expected, the molar volumes of natural magmatic liquids decrease systematically with increasing abundance of TO_3 and TO_4 units in the melts. No apparent correlation exists between molar volume and the abundance of T_2O_5 units in the magmatic liquids. Comparable linear relations exist between molar volume of X_{TO_2} units in binary metal oxide-

367 Rhyolite
1987 Andesite
287 Tholeiite &
    Olivine tholeiite
266 Basanite &
    basanitoid
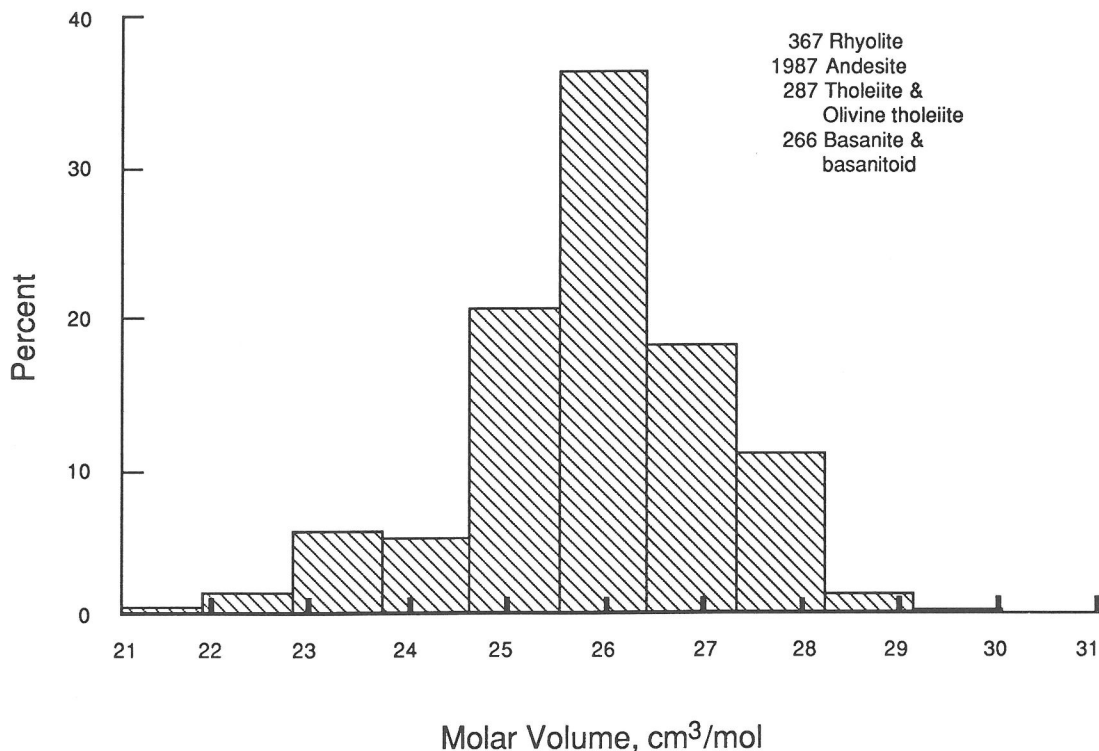
FIG. 15. Distribution of calculated molar volume (cm³/mol) for melts of major types of extrusive rocks used in Figure 19. Molar volumes were calculated from the partial molar volume data of BOTTINGA *et al.* (1983). (CHAYES, 1975a,b; 1985; see also discussion in text).
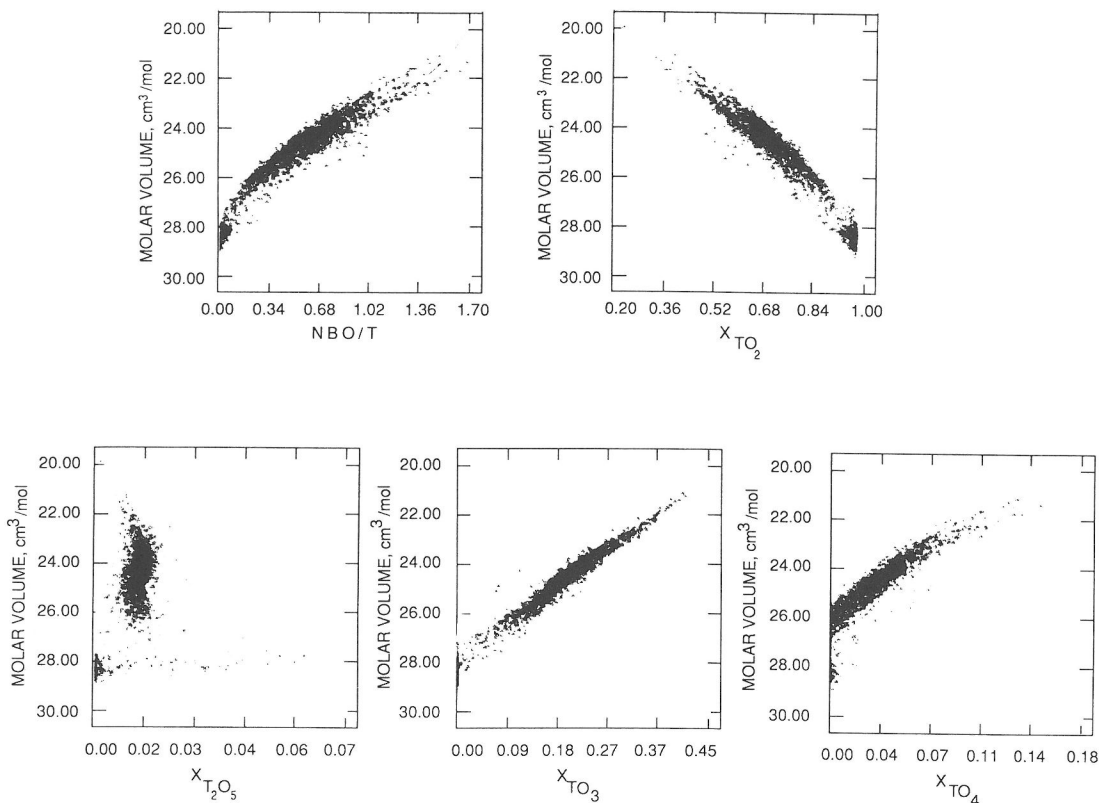
FIG. 16. Relations between bulk melt NBO/T, proportions of structural units and molar volume of melts of major extrusive rock types. Molar volumes were calculated from the partial molar volume data of BOTTINGA *et al.* (1983). (CHAYES, 1975a,b; 1985; see also discussion in text).

silica melts (BOCKRIS and KOJONEN, 1960; ROBINSON, 1969; MYSEN, 1986). It appears, therefore, that the proportion of three-dimensional network-units is the principal structural control of the molar volume of natural magmatic liquids and that the molar volumes may be estimated provided that the X_{TO_2} value is known.

One-bar viscous properties of magmatic liquids may be approximated with the model for calculation published by BOTTINGA and WEILL (1972). The distribution of viscosity η and activation energies of viscous flow (E_η) calculated for the same data base as the molar volumes are shown in Figure 17. The activation energies were calculated with the assumption that in the superliquidus temperature region, the E_η is independent of temperature. The apparent bimodal distribution of values is at least partly due to the fact that as for molar volumes, viscous properties of rhyolite melt tend to cluster in a group separated distinctly from other rock types, with significantly greater viscosities and activation energies of viscous flow. At 1300°C, for

example, the average viscosities ($\log_{10} \eta$; poise) for the groups of rocks are, 4.8 ± 0.3, 3.7 ± 0.5, 2.2 ± 0.2 and 1.7 ± 0.3 for rhyolite, andesite, tholeiite and basanite melts, respectively. The pronounced maximum near $\log \eta = 3.5$ (poise) is principally controlled by the large number of andesite analyses in the rockfile. Similar relationships exist for the activation energy of viscous flow (Figure 17).

As has been observed in simple binary and ternary systems (see summary of available data by MYSEN *et al.*, 1982; RICHET, 1984) there is a positive correlation between viscosity and NBO/T and activation energy of viscous flow and NBO/T of natural magmatic liquids, although there is a significant scatter in the data (Figure 18). The preexponential factor;

$$\ln \eta_0 = \ln \eta - E_\eta / RT, \qquad (11)$$

where η is viscosity, $\ln \eta_0$ the preexponential factor, E_η activation energy of viscous flow, R the gas constant and T the absolute temperature, does not correlate well with any structural factor calculated from
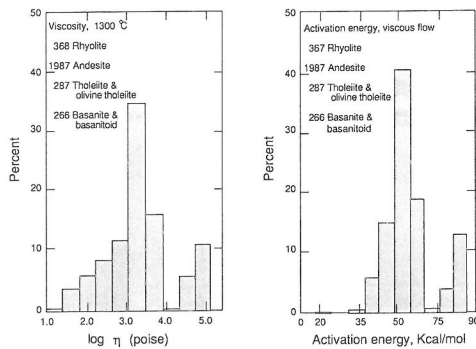
FIG. 17. Distribution of viscosity ($\log_{10} \eta$, poise at 1300°C) and activation energy of viscous flow (E_η, kcal/mol) of the melts of major extrusive rock types used in Figures 18 and 19. Viscosities and activation energies were calculated with the method of BOTTINGA and WEILL (1972) assuming Ahrrenian behavior of the melts in the superliquidus temperature region. Bulk compositions of rocktypes were extracted from rockfile RKNFSYS (CHAYES, 1975a,b; 1985).

the rock analyses. It is also noted that as has been shown for simple binary and ternary melt compositions (see BOCKRIS and REDDY, 1970; BOTTINGA and WEILL, 1972, for summary for available data), both the viscosity and the activation energies are principally functions of the proportions of three-dimensional network units in the magmatic liquids (Figure 19). As would be expected, both $\log \eta$ and E_η are negatively correlated with the proportions of TO_3 and TO_4 units in the liquids.

Redox equilibria and melt structure

It has been suggested (e.g., FUDALI, 1965; SACK et al., 1980) that the redox ratio of iron in natural magmatic liquids may be used to calculate the oxygen fugacity of equilibration if the temperature is known. To this end SACK et al., (1980) and KILINC et al., (1983) used stepwise, multiple linear regression of ferric/ferrous to incorporate temperature, oxygen fugacity, and the abundance of various oxide components. These investigators employed an expression of the form

$\ln (Fe_2O_3/FeO)$

$$= a \ln f_{O_2} + b/T + c + \sum_{i=1}^{i} d_i X_i, \quad (12)$$

where a, b, c, and d_i are regression coefficients, T is absolute temperature, $\ln f_{O_2}$ is the natural logarithm of the oxygen fugacity, and X_i are concentrations of oxide components. By fitting 57 analyses

from experimentally equilibrated liquids to this expression, SACK et al., (1980) found positive correlation of $\ln (Fe_2O_3/FeO)$ with Na_2O, K_2O, and CaO, whereas MgO, Al_2O_3, and FeO were negatively correlated. In a subsequent refinement of this treatment, KILINC et al., (1983) concluded that the ferric/ferrous depended only on CaO, Na_2O, K_2O, FeO (all positively correlated), and Al_2O_3 (which remained negatively correlated; Table 6). KILINC et al., (1983) concluded that Fe_2O_3/FeO was independent of MgO content of the liquid. Magnesium oxide was not identified as a variable in the experimental results reported by THORNBER et al., (1980).

There were significant bulk compositional differences between the samples used by THORNBER et al., (1980), SACK et al., (1980), and KILINC et al., (1983). Whereas THORNBER et al., (1980) employed mostly basaltic liquids, with selective addition of specific oxides, SACK et al., (1980) and KILINC et al., (1983) reported laboratory-calibrated $Fe^{3+}/\Sigma Fe$ with a wide range of bulk compositions from mafic to felsic.

The discrepancies between these data sets most probably arise from the fact that in neither treatment of the whole-rock analyses were the structural roles of the cations and the structural positions of ferric and ferrous iron considered. The limitation of this approach was evident in the disagreement between the functional relationships of the various oxide components depending on temperature, oxygen fugacity, and bulk composition itself (SACK et al., 1980; THORNBER et al., 1980; KILINC et al., 1983). The standard errors of the regression coefficients (Table 6) were also quite large, suggesting that regression of $\ln (Fe_2O_3/FeO)$ against the metal oxides does not result in the best possible relationship between redox state and melt composition.

With the structural information discussed above, the approach suggested by SACK et al., (1980) may be refined and stepwise linear regression may be applied to a rock composition after it has been recast to the relevant structural components. The structural components are those found to govern $Fe^{3+}/\Sigma Fe$ in binary and ternary systems. It is suggested that the expression of the form

$$\ln (Fe^{2+}/Fe^{3+}) = a + 10^4 b/T + c \ln f_{O_2}$$
$$+ d[Al/(Al + Si)] + e[Fe^{3+}/(Fe^{3+} + Si^{4+})]$$
$$+ \sum_{j=1}^{j} f_j (NBO/T)_j \quad (13)$$

can be used to describe the relationship between Fe^{2+}/Fe^{3+}, temperature, oxygen fugacity and melt
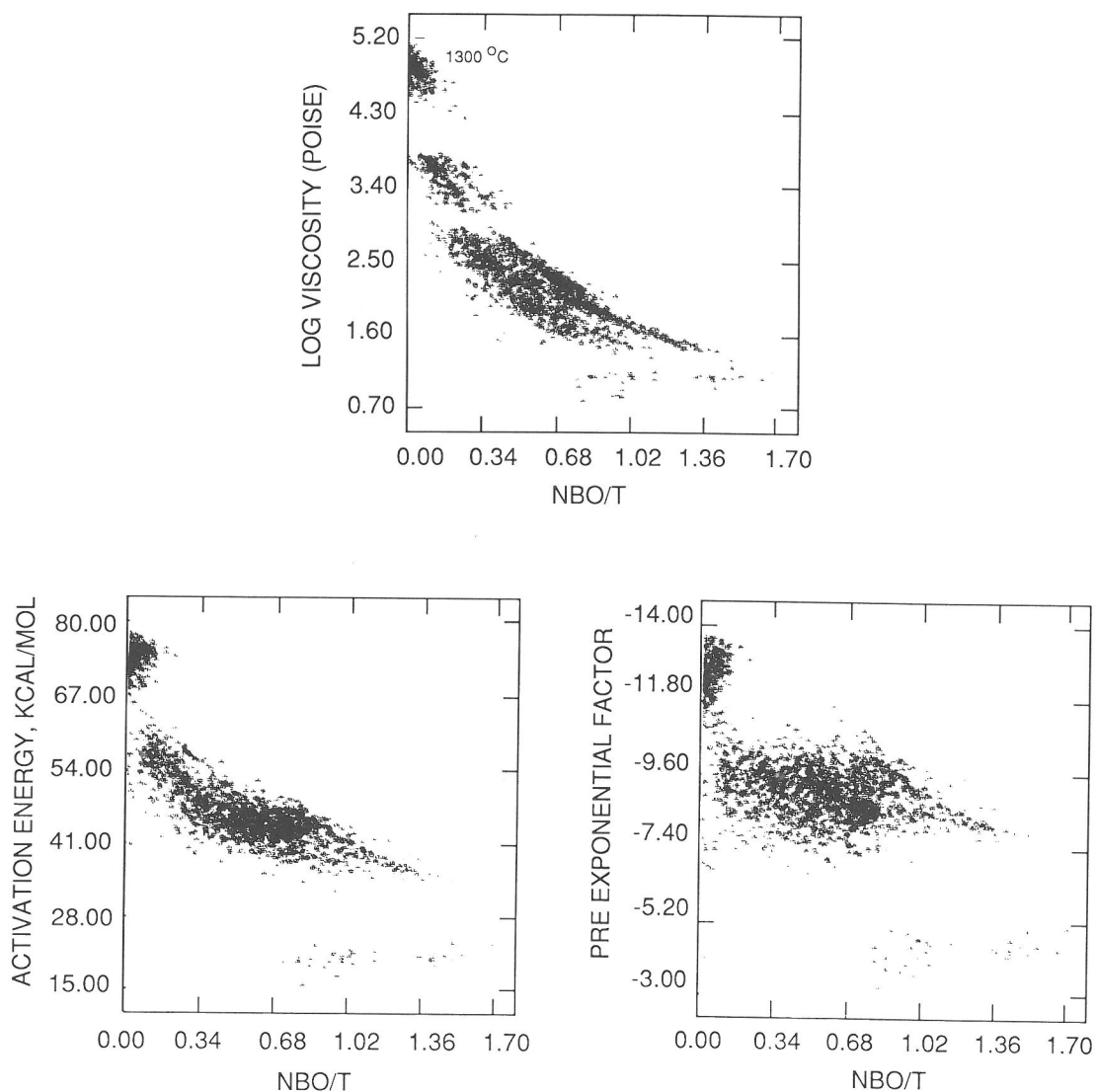
FIG. 18. Viscosity and activation energy of viscous flow of melts of major extrusive rocktypes as a function of NBO/T of the melts. Viscosities and activation energies were calculated with the method of BOTTINGA and WEILL (1972) assuming Ahrrenian behavior of the melts in the superliquidus temperature region. Bulk compositions of rocktypes were extracted from rockfile RKNFSYS (CHAYES, 1975a,b; 1985).

structure. The f_j and $(NBO/T)_j$ are the regression coefficients and NBO/T values for the individual network-modifying oxides, respectively. The coefficients a, b, c, and d together with f_j are obtained with stepwise linear regression. The expression in equation (13) takes into account each of the variables identified as independent variables affecting $Fe^{3+}/\Sigma Fe$. This treatment differs from that resulting in equation (12), where no decision was made in regard to which structural variables influence $Fe^{3+}/\Sigma Fe$.

Linear regression has been carried out with 267 experimental calibrations of $Fe^{3+}/\Sigma Fe$ in simple melt systems (only binary metal oxide and ternary metal oxide-alumina-silica systems). The resulting coefficients are shown in Table 7 and are compared with those obtained by similar regression of available data for laboratory-calibrated, natural rock
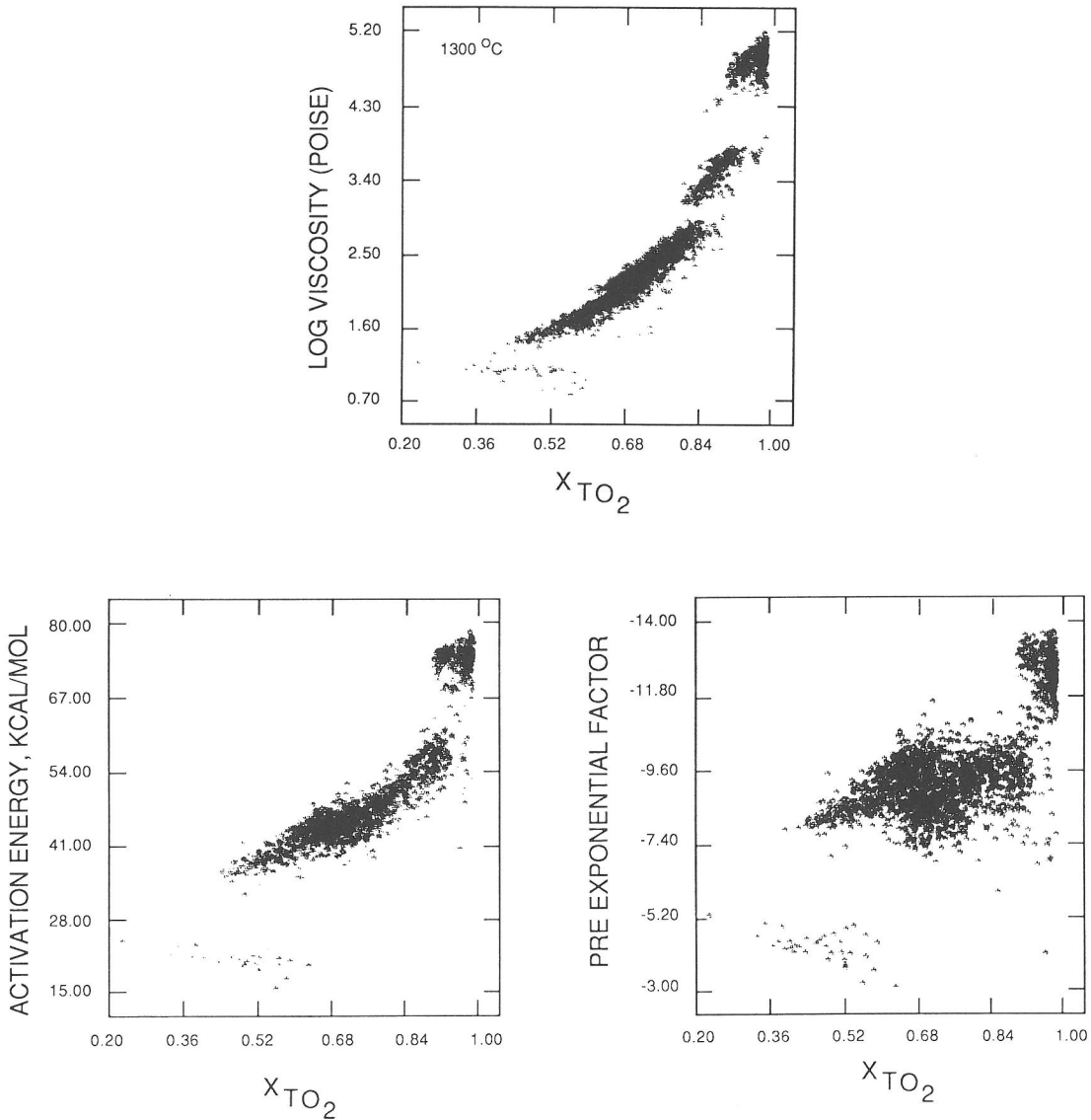
FIG. 19. Viscosity and activation energy of viscous flow of melts of major extrusive rock types as a function of abundance of structural units (A, X_{TO_2}; B, X_{TO_3}) in the melts. Viscosities and activation energies were calculated with the method of BOTTINGA and WEILL (1972) assuming Ahrrenian behavior of the melts in the superliquidus temperature region. Bulk compositions of rocktypes were extracted from rockfile RKNFSYS (CHAYES, 1975a,b; 1985).

compositions as well as compositions in simple systems (KENNEDY, 1948; FUDALI, 1965; SACK et al., 1980; KILINC et al., 1983; THORNBER et al., 1980) with a total of 460 analyses. Finally, the redox ratios of both groups of compositions were regressed against melt structural parameters according to equation (13) (a total of 460 analyses). In each of these sets of coefficients, the standard errors are sig-

nificantly smaller than those found from oxide components (SACK et al., 1980; KILINC et al., 1983). Thus, regression of ln (Fe^{2+}/Fe^{3+}) against independently established melt structural factors yields a more reliable formulation than one based on empirical relationships between redox ratio and oxide contents of the melts.

It is evident from this exercise that among the
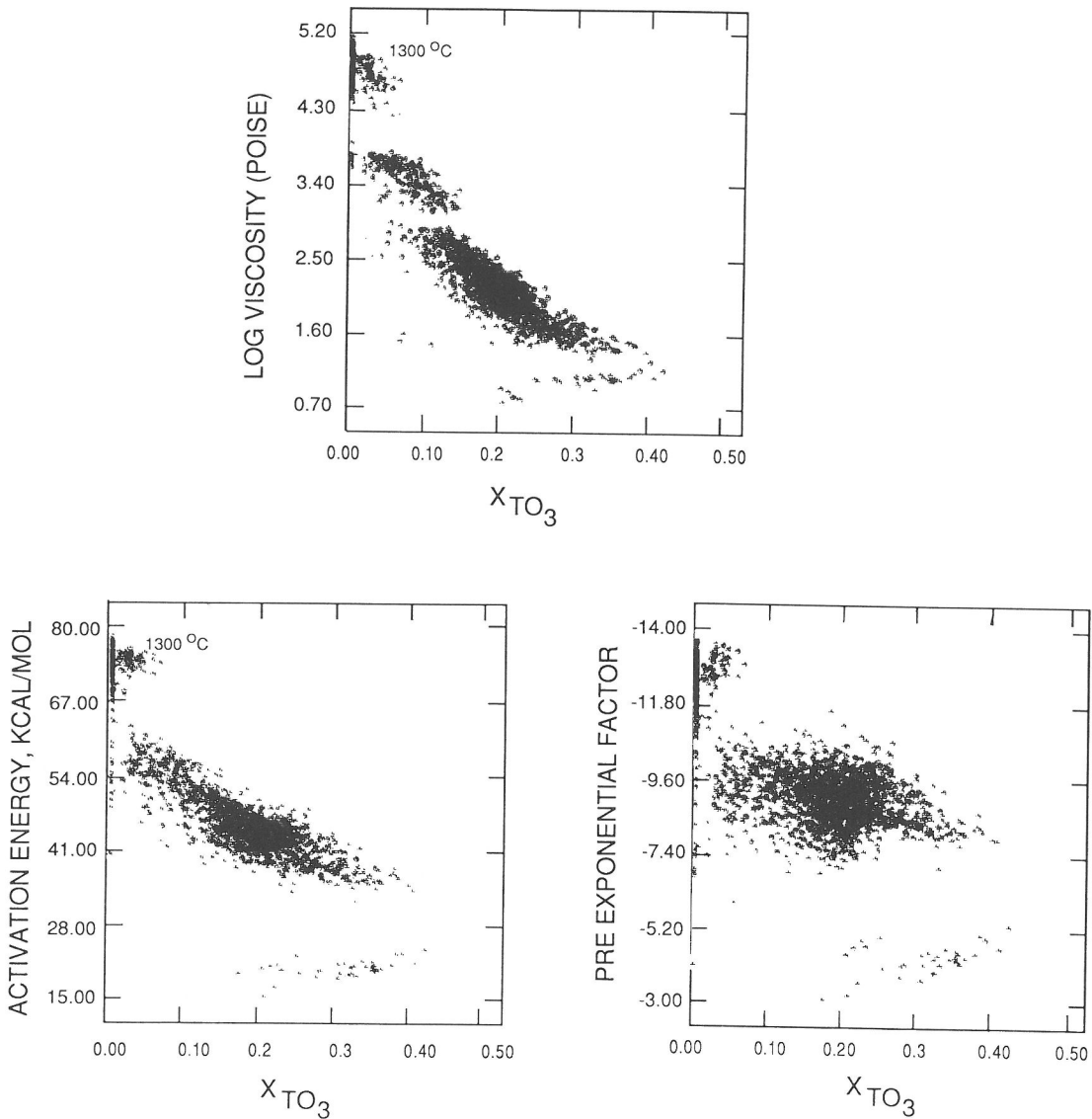
FIG. 19. (Continued)

network-modifying cations the ln (Fe^{2+}/Fe^{3+}) is negatively correlated with the proportion of non-bridging oxygen associated with Ca^{2+}, Na^+, and Fe^{2+} (Table 7). A negative but less reliable correlation also exists in some of the data summarized in Table 6 (KILINC *et al.,* 1983). All three analyses show that Fe^{2+}/Fe^{3+} *increases* with increasing NBO/T associated with Mg^{2+}. It is not clear why Mg^{2+} is an exception among the network-modifying cations in this respect. There is also a rapid decrease in ln (Fe^{2+}/Fe^{3+}) with increasing $Fe^{3+}/(Fe^{3+} + Si^{4+})$. In the case of the simple-system calibration, as well as that based on all analyses, the ln (Fe^{2+}/Fe^{3+}) will decrease with increasing $Al/(Al + Si)$ (with all Al^{3+} charge-balanced in tetrahedral coordination), but the coefficient obtained by regression with only the natural rock compositions has the opposite sign. Although there is no obvious explanation for this apparent difference, it should be remembered that the range in $Al/(Al + Si)$ in the natural rock compositions is relatively small (0.15–0.25), whereas for the simple-system calibration, the range covered is

B. O. Mysen

Table 6. Regression coefficients with standard errors ($\pm 1\sigma$) for Equation (12)

Coefficient	SACK et al. (1980)		KILINC et al. (1983)	
	Value	Standard error	Value	Standard error
a	0.218	0.007	0.219	0.004
b	13,184.7	959.0	12,670.0	900.0
c	−4.50	3.04	−7.54	0.55
$d_{Al_2O_3}$	−2.15	2.88	−2.24	1.03
d_{FeO} *	−4.50	3.69	1.55	1.03
d_{MgO}	−5.44	3.04	—	—
d_{CaO}	0.07	3.08	2.96	0.53
d_{Na_2O}	3.54	3.97	8.42	1.41
d_{K_2O}	4.19	4.12	9.59	1.45

* Total iron oxide as FeO.

between 0 and 0.43. More reliance is placed, therefore, on this latter analysis.

The coefficients in Table 7 may be inserted in equation (13), and this equation may be used, for example, as an oxygen-fugacity barometer. The calculated f_{O_2} values for the samples in the data set are compared with the measured values in Figure 20. From this comparison it is evident that as an oxygen-fugacity barometer of natural igneous rocks based only on the simple-system calibration, 40% of the calculated values are within ± 0.5 log unit and 67% are within ± 1.0 log unit of f_{O_2}. Between 85 and 90% of the calculated values are within ± 1.5 log units of the measured value (Figure 20a). When the whole data set of simple-system and natural melt compositions is employed (see Table 7), the deviation from measured values is smaller (Figure 20b), and 54% of the analyses are within ± 0.5 log unit

of oxygen fugacity and 85%, within ± 1.0 log unit. About 95% fall within ± 1.5 log units. It is suggested that this model relating redox ratios of iron to temperature, oxygen fugacity, and melt structure is an adequate description and that equation (13), with the coefficients in Table 7, can be used with confidence to calculate oxygen-fugacity conditions of natural magmatic liquids at 1 atmosphere. Although some of the principles governing the pressure dependence of ferric/ferrous have been established (MO et al., 1982; MYSEN and VIRGO, 1983), the data base is at present insufficient to extend this treatment to high pressure.

SUMMARY

Available experimental data from model system melt structure studies have been used to describe

Table 7. Regression coefficients for Equation (13)

	Simple system		Natural rocks		All analyses	
	Coefficient	Standard error	Coefficient	Standard error	Coefficient	Standard error
a (const.)	10.814	1.134	4.384	0.524	15.437	0.786
b $(1/T)$	−1.989	0.203	−0.9077	0.0915	−2.848	0.138
c $(\ln f_{O_2})$	−0.3210	0.0117	−0.1420	0.0081	−0.3484	0.0120
d $[Al^{3+}/(Al^{3+} + Si)]$	−1.535	0.467	1.621	0.418	−1.309	0.469
e $[Fe^{3+}/(Fe^{3+} + Si)]$	−4.067	0.985	−9.875	0.952	−2.121	1.055
$(NBO/T)^{Mg}$	0.494	0.134	0.8607	0.2093	0.6662	0.0966
f_i $(NBO/T)^{Ca}$	−0.5228	0.1095	−0.6560	−0.1617	−0.5255	0.1084
$(NBO/T)^{Na}$	−1.584	0.238	−1.194	0.5112	−1.125	0.1790
$(NBO/T)^{Fe^{2+}}$	−1.951	0.507	−2.310	0.422	−3.215	0.538

Number of analyses in regression: simple systems, 267; natural rocks, 193; all analyses, 460.
Experimental data for regression from KENNEDY (1948), FUDALI (1965), SACK et al. (1980), THORNBER et al. (1980), KILINC et al. (1983), SEIFERT et al. (1979), VIRGO et al. (1981), MYSEN and VIRGO (1983), VIRGO and MYSEN (1985), MYSEN et al. (1980b, 1984, 1985b,c).
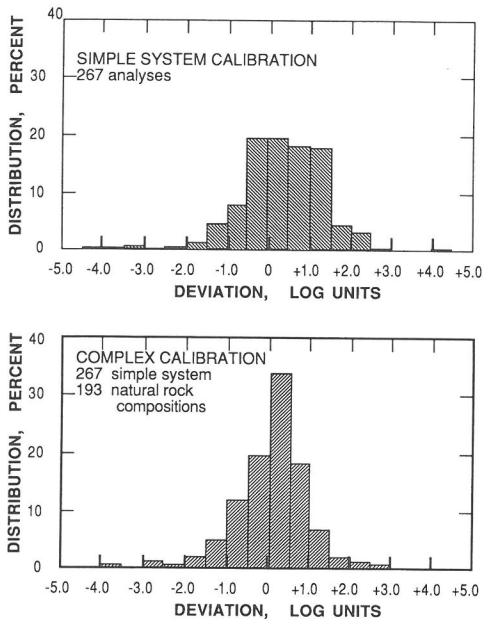
FIG. 20. Distribution of calculated oxygen fugacity from equation (13) and coefficients from Table 7 based on calibration with 267 experimental data points in simple model systems (a) and 460 experimental data points including both simple model systems and natural melt compositions (b).

the major structural features of natural magmatic liquids. These results can be used to characterize relationships between the structure of the magmatic liquid and molar volume as well as viscous behavior. The redox relations of iron can also be quantitatively described.

REFERENCES

BOCKRIS J. O'M. and KOJONEN F. (1960) The compressibility of certain molten alkali silicates and borates. *J. Amer. Chem. Soc.* **82**, 4493–4497.

BOCKRIS J. O'M. and REDDY A. K. N. (1970) *Modern Electrochemistry,* Vol. 1, 622 pp. Plenum Press.

BOTTINGA Y. and WEILL D. F. (1972) The viscosity of magmatic silicate liquids: A model for calculation. *Amer. J. Sci.* **272**, 438–475.

BOTTINGA Y., RICHET P. and WEILL D. F. (1983) Calculation of the density and thermal expansion coefficient of silicate liquids. *Bull. Mineral.* **106**, 129–138.

BRAWER S. A. and WHITE W. B. (1975) Raman spectroscopic investigation of the structure of silicate glasses.

I. The binary silicate glasses. *J. Chem. Phys.* **63**, 2421–2432.

BRAWER S. A. and WHITE W. B. (1977) Raman spectroscopic investigation of the structure of silicate glasses. II. The soda-alkaline earth-alumina ternary and quarternary glasses. *J. Non-Cryst. Solids* **23**, 261–278.

BROWN G. E., GIBBS G. V. and RIBBE P. H. (1969) The nature and variation in length of the Si-O and Al-O bonds in framework silicates. *Am. Mineral.* **54**, 1044–1061.

CALAS G. and PETIAU J. (1983) Structure of oxide glasses: Spectroscopic studies of local order and crystallochemistry: Geochemical implications. *Bull. Mineral.* **106**, 33–55.

CHANDRASEKHAR H. R., CHANDRASEKHAR M. and MANGNHANI M. H. (1979) Phonons in titanium-doped vitreous silica. *Solid State Commun.* **31**, 329–333.

CHAYES F. (1975a) A world data base for igneous petrology. *Carnegie Inst. Wash. Yearb.* **74**, 549–550.

CHAYES F. (1978b) Average composition of the commoner cenozoic volcanic rocks. *Carnegie Inst. Wash. Yearb.* **74**, 547–549.

CHAYES F. (1985) Version NTRM2 of system RKNFSYS. Unpubl. document, Geophys. Lab., Carnegie Inst. Wash., Washington DC.

DICKENSON M. P. and HESS P. C. (1981) Redox equilibria and the structural role of iron in aluminosilicate melts. *Contrib. Mineral. Petrol.* **78**, 352–358.

DICKENSON M. P. and HESS P. C. (1986) The structural role and homogenous redox equilibria of iron in peraluminous, metaluminous and peralkaline silicate melts. *Contrib. Mineral. Petrol.* **92**, 207–217.

DICKINSON J. E. and HESS P. C. (1985) Rutile solubility and titanium coordination in silicate melts. *Geochim. Cosmochim. Acta* **49**, 2289–2296.

DOMINE F. and PIRIOU B. (1986) Raman spectroscopic study of the SiO₂-Al₂O₃-K₂O vitreous system: Distribution of silicon and second neighbors. *Amer. Mineral.* **71**, 38–50.

FOX K. E., FURUKAWA T. and WHITE W. B. (1982) Luminescence of Fe³⁺ in metaphosphate glass: evidence for four- and six-coordinated sites. *J. Amer. Ceram. Soc.* **64**, C42–C43.

FRASER D. G., RAMMENSEE W. and JONES R. H. (1983) The mixing properties of melts in the system NaAlSi₂O₆-KAlSi₂O₆ as determined by Knudsen cell mass spectrometry. *Bull. Mineral.* **106**, 111–117.

FRASER D. G. and BOTTINGA Y. (1985) The mixing properties of melts and glasses in the system NaAlSi₃O₈-KAlSi₃O₈: Comparison of experimental data obtained by Knudsen cell mass spectrometry and solution calorimetry. *Geochim. Cosmochim. Acta* **49**, 1377–1381.

FUDALI F. (1965) Oxygen fugacity of basaltic and andesitic magmas. *Geochim. Cosmochim. Acta* **29**, 1063–1075.

FURUKAWA T. and WHITE W. B. (1979) Structure and crystallization of glasses in the Li₂Si₂O₅-TiO₂ system determined by Raman spectroscopy. *Phys. Chem. Glasses* **20**, 69–80.

FURUKAWA T., FOX K. E. and WHITE W. B. (1981) Raman spectroscopic investigation of the structure of silicate glasses. III. Raman intensities and structural units in sodium silicate glasses. *J. Chem. Phys.* **15**, 3226–3237.

GALEENER F. L. and MIKKELSEN J. C. (1979) The Raman spectra and structure of pure vitreous P₂O₅. *Solid State Commun.* **20**, 505–510.

GIBBS G. V., MEAGHER E. P., NEWTON M. D. and SWANSON D. K. (1981) A comparison of experimental and theoretical bond length and angle variations for minerals and inorganic solids, and molecules. In *Structure and Bonding in Crystals* (editors M. O'KEEFE and A. NAVROTSKY), Vol. 2, Chap. 9, Academic Press.

HOCHELLA M. F. and BROWN G. E. (1985) Structure and viscosity of rhyolite composition melt. *Geochim. Cosmochim. Acta* **49**, 2631–2640.

KENNEDY G. C. (1948) Equilibrium between volatiles and iron oxides in rocks. *Amer. J. Sci.* **246**, 529–549.

KILINC A., CARMICHAEL I. S. E., RIVERS M. L. and SACK R. O. (1983) The ferric-ferrous ratio of natural silicate liquids equilibrated in air. *Contrib. Mineral. Petrol.* **83**, 136–141.

KUSHIRO I. (1975) On the nature of silicate melt and its significance in magma genesis: Regularities in the shift of liquidus boundaries involving olivine pyroxene, and silica materials. *Amer. J. Sci.* **275**, 411–431.

LAUER H. V. (1977) Effect of glass composition on major element redox equilibria: Fe^{2+}-Fe^{3+}. *Phys. Chem. Glasses* **18**, 49–52.

MATSON D. W., SHARMA S. K. and PHILPOTTS J. A. (1983) The structure of high-silica alkali-silicate glasses—A Raman spectroscopic investigation. *J. Non-Cryst. Solids* **58**, 323–352.

MCMILLAN P. (1984) Structural studies of silicate glasses and melts—applications and limitations of Raman spectroscopy. *Amer. Mineral.* **69**, 622–644.

MCMILLAN P., PIRIOU B. and NAVROTSKY A. (1982) A Raman spectroscopic study of glasses along the joins silica-calcium aluminate, silica-sodium aluminate, and silica-potassium aluminate. *Geochim. Cosmochim. Acta* **46**, 2021–2037.

MO X. X., CARMICHAEL I. S. E., RIVERS M. and STEBBINS J. (1982) The partial molar volume of Fe_2O_3 in multicomponent silicate liquids and the pressure dependence of oxygen fugacity in magmas. *Mineral. Mag.* **45**, 237–245.

MYSEN B. O. (1986) Structure and petrologically important properties of silicate melts relevant to natural magmatic liquids. In *Short Course in Silicate Melts,* (editor C. M. SCARFE), Chap. 7, pp. 180–209, Mineral. Soc. Canada.

MYSEN B. O. and VIRGO D. (1978) Influence of pressure, temperature, and bulk composition on melt structures in the system $NaAlSi_2O_6$-$NaFe^{3+}Si_2O_6$. *Amer. J. Sci.* **278**, 1307–1322.

MYSEN B. O. and VIRGO D. (1980) Trace element partitioning and melt structure: An experimental study at 1 atm. pressure. *Geochim. Cosmochim. Acta* **44**, 1917–1930.

MYSEN B. O. and VIRGO D. (1983) Redox equilibria, structure and melt properties in the system Na_2O-Al_2O_3-SiO_2-Fe-O. *Carnegie Inst. Wash. Yearb.* **82**, 313–317.

MYSEN B. O. and VIRGO D. (1985) Iron-bearing silicate melts: relations between pressure and redox equilibria. *Phys. Chem. Mineral.* **12**, 191–200.

MYSEN B. O., SEIFERT F. A. and VIRGO D. (1980a) Structure and redox equilibria of iron-bearing silicate melts. *Amer. Mineral.* **65**, 867–884.

MYSEN B. O., VIRGO D. and SCARFE C. M. (1980b) Relations between the anionic structure and viscosity of silicate melts—a Raman spectroscopic study. *Amer. Mineral.* **65**, 690–710.

MYSEN B. O., RYERSON F. J. and VIRGO D. (1980c) The influence of TiO_2 on structure and derivative properties of silicate melts. *Amer. Mineral.* **65**, 1150–1165.

MYSEN B. O., VIRGO D. and KUSHIRO I. (1981a) The structural role of aluminum in silicate melts—A Raman spectroscopic study at 1 atmosphere. *Amer. Mineral.* **66**, 678–701.

MYSEN B. O., RYERSON F. and VIRGO D. (1981b) The structural role of phosphorous in silicate melts. *Amer. Mineral.* **66**, 106–117.

MYSEN B. O., VIRGO D. and SEIFERT F. A. (1982) The structure of silicate melts: Implications for chemical and physical properties of natural magma. *Rev. Geophys.* **20**, 353–383.

MYSEN B. O., VIRGO D. and SEIFERT F. A. (1984) Redox equilibria of iron in alkaline earth silicate melts: Relationships between melt structure, oxygen fugacity, temperature and properties of iron-bearing silicate liquids. *Amer. Mineral.* **69**, 834–848.

MYSEN B. O., VIRGO D. and SEIFERT F. A. (1985a) Relationships between properties and structure of aluminosilicate melts. *Amer. Mineral.* **70**, 834–847.

MYSEN B. O., VIRGO D., NEUMANN E.-R. and SEIFERT F. A. (1985b) Redox equilibria and the structural states of ferric and ferrous iron in melts in the system CaO-MgO-Al_2O_3-SiO_2: Relations between redox equilibria, melt structure and liquidus phase equilibria. *Amer. Mineral.* **70**, 317–322.

MYSEN B. O., VIRGO D., SCARFE C. M. and CRONIN D. J. (1985c) Viscosity and structure of iron- and aluminum-bearing calcium silicate melts. *Amer. Mineral.* **70**, 487–498.

NAVROTSKY A., HON R., WEILL D. F. and HENRY D. J. (1980) Thermochemistry of glasses and liquids in the systems $CaMgSi_2O_6$-$CaAl_2SiO_6$-$NaAlSi_3O_8$, SiO_2-$CaAl_2Si_2O_8$-$NaAlSi_3O_8$, and SiO_2-Al_2O_3-CaO-Na_2O. *Geochim. Cosmochim. Acta* **44**, 1409–1433.

NAVROTSKY A., PERAUDEAU P., MCMILLAN P. and COUTOURES J. P. (1982) A thermochemical study of glasses and crystals along the joins silica-calcium aluminate and silica-sodium aluminate. *Geochim. Cosmochim. Acta* **46**, 2039–2049.

NAVROTSKY A., ZIMMERMANN H. D. and HERWIG R. L. (1983) Thermochemical study of glasses in the system $CaMgSi_2O_6$-$CaAl_2SiO_6$. *Geochim. Cosmochim. Acta* **47**, 1535–1539.

NELSON B. N. and EXHAROS G. J. (1979) Vibrational spectroscopy of cation-site interactions in phosphate glasses. *J. Chem. Phys.* **71**, 2739–2747.

NELSON C. and TALLANT D. R. (1984) Raman studies of sodium silicate glasses with low phosphate contents. *Phys. Chem. Glasses* **25**, 31–39.

NOLET D. A., BURNS R. G., FLAMM S. L. and BESANCON J. R. (1979) Spectra of Fe-Ti silicate glasses: Implications to remote-sensing of planetary surfaces. *Proc. Lunar Planet. Sci. Conf. 10th,* 1775–1786.

RAY B. N. and NAVROTSKY A. (1984) Thermochemistry of charge-coupled substitutions in silicate glasses: The system $M^{n+}_{1/n} AlO_2$-SiO_2 (M = Li, Na, K, Rb, Cs, Mg, Ca, Sr, Ba, Pb). *J. Amer. Ceram. Soc.* **89**, 606–610.

RICHET P. (1984) Viscosity and configurational entropy of silicate melts. *Geochim. Cosmochim. Acta* **48**, 471–485.

RICHET P. and BOTTINGA Y. (1985) Heat capacity of aluminum-free liquid silicates. *Geochim. Cosmochim. Acta* **49**, 471–486.

RICHET P. and BOTTINGA Y. (1986) Thermochemical properties of silicate glasses and liquids: A review. *Rev. Geophys.* **24**, 1–26.

ROBINSON H. A. (1969) Physical properties of alkali silicate

glasses: I. Additive relations in alkali binary glasses. *J. Amer. Ceram. Soc.* **53**, 392–399.

RYERSON F. J. (1985) Oxide solution mechanisms in silicate melts: Systematic variations in the activity coeffient of SiO_2. *Geochim. Cosmochim. Acta* **49**, 637–651.

RYERSON F. J. and HESS P. C. (1980) The role of P_2O_5 in silicate melts. *Geochim. Cosmochim. Acta* 44, 611–625.

SACK R. O., CARMICHAEL I. S. E., RIVERS M. and GHIORSO M. S. (1980) Ferric-ferrous equilibria in natural silicate liquids at 1 bar. *Contrib. Mineral. Petrol.* **75**, 369–377.

SANDSTROM D. R., LYTLE F. W., WEI P., GREEGOR R. B., WONG J. and SCHULTZ P. (1980) Coordination of Ti in TiO_2-SiO_2 glasses by X-ray absorption spectroscopy. *J. Non-Cryst. Solids* **41**, 201–207.

SCARFE C. M. (1977) Structure of two silicate rock melts charted by infrared absorption spectroscopy. *Chem. Geol.* **15**, 77–80.

SEIFERT F. A., VIRGO D. and MYSEN B. O. (1979) Melt structures and redox equilibria in the system Na_2O-FeO-Fe_2O_3-$Al_2O_3SiO_2$. *Carnegie Inst. Wash. Yearb.* **78**, 511–519.

SEIFERT F. A., MYSEN B. O. and VIRGO D. (1982) Three-dimensional network melt structure in the systems SiO_2-$NaAlO_2$, SiO_2-$CaAl_2O_4$ and SiO_2-$MgAl_2O_4$. *Amer. Mineral.* **67**, 696–711.

TAYLOR M. and BROWN G. E. (1979a) Structure of mineral glasses. II. The SiO_2-$NaAlSiO_4$ join. *Geochim. Cosmochim. Acta* **43**, 1467–1475.

TAYLOR M. and BROWN G. E. (1979b) Structure of mineral glasses. I. The feldspar glasses $NaAlSi_3O_8$, $KAlSi_3O_8$, $CaAl_2Si_2O_8$. *Geochim. Cosmochim. Acta* **43**, 61–77.

THORNBER C. R., ROEDER P. L. and FOSTER J. R. (1980) The effect of composition on the ferric-ferrous ratio in basaltic liquids at atmospheric pressure. *Geochim. Cosmochim. Acta* **44**, 525–533.

TOBIN M. C. and BAAK T. (1968) Raman spectra of some low-expansion glasses. *J. Opt. Soc. Amer.* **58**, 1459–1460.

VERWEIJ H. (1979a) Raman study of the structure of alkali germanosilicate glasses. I. Sodium and potassium metagermanosilicate glasses. *J. Non-Cryst. Solids* **33**, 41–53.

VERWEIJ H. (1979b) Raman study of the structure of alkali germanosilicate glasses. II. Lithium, sodium and potassium digermanosilicates glasses. *J. Non-Cryst. Solids* **33**, 55–69.

VIRGO D. and MYSEN B. O. (1985) The structural state of iron in oxidized vs. reduced glasses at 1 atm.: a ^{57}Fe Mossbauer study. *Phys. Chem. Mineral.* **12**, 65–76.

VIRGO D., MYSEN B. O. and KUSHIRO I. (1980) Anionic constitution of silicate melts quenched at 1 atm from Raman spectroscopy: Implications for the structure of igneous melts. *Science* **208**, 1371–1373.

VIRGO D., MYSEN B. O. and SEIFERT F. A. (1981) Relationship between the oxidation state of iron and structure of silicate melts. *Carnegie Inst. Wash. Yearb.* **80**, 308–311.

VISSER W. and VAN GROOS A. F. KOSTER (1979) Effects of P_2O_5 and TiO_2 on the liquid-liquid equilibria in the system K_2O-FeO-Al_2O_3-SiO_2. *Amer. J. Sci.* **279**, 970–988.

WATSON E. B. (1976) Two-liquid partition coefficients: Experimental data and geochemical implications. *Contrib. Mineral. Petrol.* **56**, 119–134.